J. Fluid Mech. (1981), *vol.* 105, *pp.* 19–59
Printed in Great Britain

Experimental evidence for the existence of the 'mesolayer' in turbulent systems

By ROBERT R. LONG AND TIEN-CHAY CHEN

Department of Earth and Planetary Sciences,
The Johns Hopkins University,
Baltimore, Maryland 21218

(Received 18 June 1980)

The paper is a study of experimental data in the light of new theories of turbulence recently developed by the first author for a number of problems including flow in a pipe, boundary layer at zero incidence, atmospheric boundary layer, turbulent convection and distribution of energy in wavenumber space in decaying, isotropic turbulence. In each of these, a basic element is a 'mesolayer' or 'mesoregion' in physical space or wavenumber space which is absent in earlier theories and which intrudes between the inner and outer regions preventing the overlap assumed in the derivation of the classical results, e.g. the logarithmic profile in shear flow. The new and old theories differ both in principle and in the final results: the new ideas replace rather than modify or extend the older ones.

The main purpose of this paper is to bring together accumulated evidence concerning the mesolayer theories. We believe that this evidence provides overwhelming support for the existence of the mesolayer and for its pervasive importance in problems of turbulence.†

1. Introduction

One of us (R.R.L.) has recently developed new concepts in the theory of turbulent motion for individual problems, namely turbulent flow in a pipe, turbulent flow in a boundary layer at zero incidence, the turbulent atmospheric boundary layer, turbulent convection and the energy spectrum at large wavenumbers in isotropic, decaying turbulence.

The basic ingredient in these theories is a new boundary layer, which we call the *mesolayer* (and a new region in wavenumber space called the *mesoregion*). These regions have escaped notice, in general, although they resemble the laminar boundary layer on a flat plate (Batchelor 1967, p. 309) or, in turbulence, the viscous layer in the so-called shear-free turbulence of Uzkan & Reynolds (1967), Thomas & Hancock (1977) and Hunt & Graham (1978). The mesolayer makes a fundamental change in the existing theories of turbulence. The purpose of this paper is to present all data we

† *Editorial footnote.* Although the referees were not persuaded that the claims for the 'new theories of turbulence', made by the authors in the abstract and elsewhere in this paper, are justified, we think that publication in the *Journal* may serve a useful purpose. The authors have assembled a large body of data for various turbulent flow systems. These data should enable readers to test different aspects of the 'classical' and 'new' theories for themselves and should stimulate thought about the foundations of the classical ideas and about extensions of these ideas, as well as about the validity of the new theories.

have so far found relevant to the existence of the mesolayer. The title suggests that this evidence supports the theory. It does, but we do not suppress contrary evidence. In fact, we have found no data which conflict with the predictions of the theory in any important way.

The theories yield behaviours of various mean quantities as functions of space or wavenumber, but only upon the assignment of universal constants. Actually, where it is possible to make comparisons, the constants may be chosen to afford excellent agreement with the data. But despite the fact that such agreement has long been accepted as verification of the logarithmic and $k^{-\frac{5}{3}}$ profiles, the fashion in recent years is to require more than this for publication of new theories (as if in reluctance to contemplate the possibility that these mainstays of turbulence wisdom are wrong), and so we concentrate here on more severe tests of our predictions. For the most part, we look into the theories for measurable, direct manifestations of the existence of the mesolayer and verify that the locations of these vary with the predicted location of the mesolayer.

More detailed papers (Long 1980*a–d*; Chern & Long 1980) on the particular applications of mesolayer theory specified in the first paragraph of this section are available, and may be obtained direct on request from the authors.

2. Comments on classical theory

We begin with some general comments on existing theory (which we call 'classical') of turbulent shear flow at high Reynolds numbers near a wall. The basic ideas were developed long ago by von Kármán (1930), Prandtl (1925, 1932), and are set forth in the basic textbooks, for example Monin & Yaglom (1971), Tennekes & Lumley (1972), and Hinze (1975). The theory contains three basic assumptions. The first, called 'the universal law of the wall', is that a region exists near the wall where mean quantities are functions only of viscosity ν, friction velocity u_τ and distance from the wall z_d, where we use the subscript d to indicate dimensional quantities. The law of the wall, pertaining to mean velocity, for example, is

$$\overline{u} = \overline{u}_+(z), \tag{1}$$

where $z = u_\tau z_d/\nu$ and where, throughout the paper, we scale generally on u_τ and ν. We need not doubt that this assumption is correct. In the first place it is a very mild hypothesis. For example, if one pictures an infinite smooth plate put in motion parallel to itself by the imposition of a stress per unit area ρu_τ^2, the assumption of the law of the wall amounts, merely, to accepting that the mean velocity relative to the wall at a fixed distance above the plate ultimately becomes steady so that time, proportional in this case to the outer length, does not enter the problem in a region near the wall. In turbulent flow in a pipe the law of the wall assumes merely that the mean velocity at a fixed value of z becomes independent of the radius of the pipe a as $a \to \infty$, holding the friction velocity fixed. In any case, the assumption has been verified in all experiments in pipes and boundary layers, e.g. Laufer (1954), and in many other types of flows. Laufer's data, for example, indicate that all mean curves, scaled on u_τ and ν, collapse into a single curve in a region near the wall whatever the size of the Reynolds number R, although the collapse occurs in regions of various thicknesses depending, somewhat, on the mean quantity being measured. For example,

the region of the law of the wall for the root-mean-square streamwise velocity in a pipe is perhaps one-half the thickness of the same region for the root-mean-square normal velocity (Laufer 1954; Lawn 1971). We will offer an explanation for this later.

The second assumption of classical theory (von Kármán 1930; Townsend 1976, p. 133) is 'Reynolds number similarity', which assumes that a region exists far from the wall where, to first approximation, dimensional forms of mean quantities are independent of ν and so depend only on u_τ, H and z_d, where H is the outer length, e.g. the thickness of the boundary layer or the radius of the pipe. Care is required here because experiment indicates that mean quantities having an intimate connection with the *small scales* of the turbulent motion (fine structure) in fact vary with the viscosity in the outer region. We illustrate by considering the energy equation in shear flow. One term is a generation term $T\overline{u}_z$, where T is the Reynolds stress, $T = -\overline{u'w'}$, and another is the dissipation ϵ. The dimensional forms of Reynolds stress and mean velocity gradient conform to Reynolds numbers similarity as shown in countless experiments, for example Fritsch (1928), Laufer (1954) and Perry & Abell (1975). Not surprisingly then, the dimensional dissipation function ϵ_d also obeys Reynolds number similarity because the generation and the dissipation terms balance closely in the outer region. But notice that

$$\epsilon_d \sim \nu\overline{(\nabla_d u_d')^2} \tag{2}$$

and therefore that $\overline{(\nabla_d u_d')^2}$, though also a mean quantity, is *inversely proportional to the viscosity in the outer region and does not obey Reynolds number similarity.* Of course, derivatives in turbulent flows, and the mean velocity itself are influenced by viscosity, and we must be careful not to require that they conform to Reynolds number similarity. If we keep this in mind, however, independence of ν is not only an excellent assumption as a practical matter but probably is also asymptotically correct as viscosity tends to zero and we so assume.

The third assumption of classical theory is an overlap of the inner and outer regions at large R implying that mean quantities are independent of both ν and H in the overlap region. To many, the assumption of the existence of an overlap region seems so obvious that little or no discussion is given of it and we have only discovered one author who seriously challenges it (Malkus 1979). Tennekes & Lumley (1972, p. 147) accept its existence but consider that the problem deserves detailed discussion. They argue (figure 1) that, although ν is important near the wall, as we move outward it should become unimportant beyond some value of z of order 1, say at $z = a_i$, where a_i is some number, perhaps $a_i = 100$. On the other hand, as we move inward from the outer region, H should become unimportant at some fixed value of z_d/H, i.e. at some z of order R. Figure 1 then shows that an overlap, indicated by the double-hatched region, will exist at high enough R. The argument is obviously correct if one accepts the limits of the inner and outer regions adopted by Tennekes & Lumley, but, seemingly, the choice of these two limits is only 'obvious' if one has faith that the overlap in fact exists!

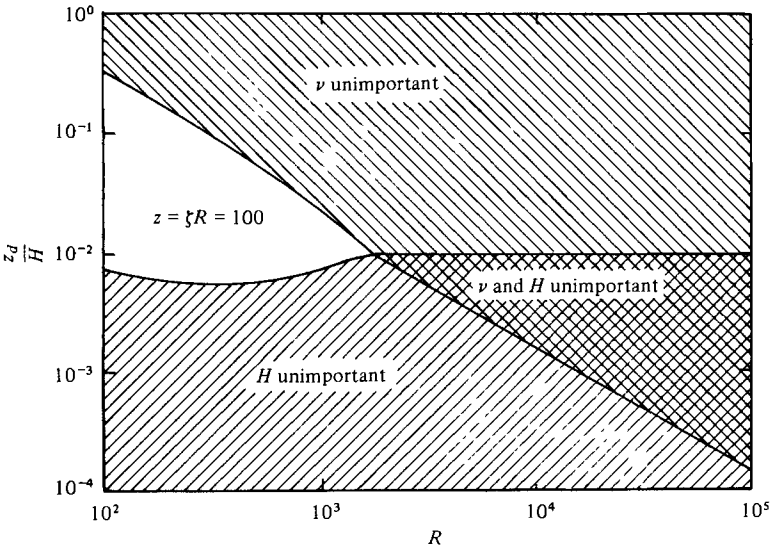

FIGURE 1. Classical concept of inner and outer regions in shear flow and the overlap region where H and ν are both unimportant. We denote the outer length by H and the Reynolds number by R. We write ζ for the ratio of distance from wall to outer length.

3. A new look at the transition region

In our initial investigations, it was observed that in the two experiments of Laufer (1954) the Reynolds stress, $T = -\overline{u'w'}$, appears to have its maximum at distances from the wall proportional to $R^{\frac{1}{2}}$. More recently, we have found nine additional points for pipe flow from Nikuradse (1932), Ueda & Mizushina (1977) and Schildknecht, Miller & Meir (1979) and two other points from experiments with a boundary layer at zero incidence (Klebanoff 1954, Gupta & Kaplan 1972). We have put them all together in figure 2 and they seem indeed to lie on a single line with a $\frac{1}{2}$-slope. Of course, more data are needed but this may be accepted as good indication of such behaviour.

There have been a number of efforts in recent years to carry the classical theory, which assumes an overlap, to higher approximations (Tennekes 1968, Yajnik 1970, Bush & Fendell 1972, 1973, 1974, Fendell 1972, Afzal & Yajnik 1973, Afzal 1976, Lund & Bush 1980). If one accepts the classical theory, it is not hard to accept also a form of the higher approximations† in which the errors in both the law of the wall and in Reynolds number similarity are of order R^{-1}. Then, by a trivial extension of the arguments of Afzal (1976), one obtains

$$S = S_{00}^{+} + S_{01}^{+} z^{-1} + S_{02}^{+} z^{-2} + \ldots + R^{-1}(S_{10}^{+} z + S_{11}^{+} + S_{12}^{+} z^{-1} + \ldots) + R^{-2}(S_{20}^{+} z^2 + S_{21}^{+} z + S_{22}^{+} + \ldots) + \ldots, \tag{3}$$

$$T = 1 - S_{00}^{+} z^{-1} - S_{01}^{+} z^{-2} - \ldots - R^{-1}(z + S_{10}^{+} + S_{11}^{+} z^{-1} + \ldots) - R^{-2}(S_{20}^{+} z + S_{21}^{+} + \ldots) - R^{-3}(S_{30}^{+} z^2 + S_{31}^{+} z + \ldots) + \ldots, \tag{4}$$

† Tennekes & Lumley (1972, p. 174) present a theory in which the second approximation to classical theory is proportional to $R^{-\frac{1}{3}}$. We have been unsuccessful in attempts to relate their work and the earlier work of Tennekes (1968) to our present efforts.

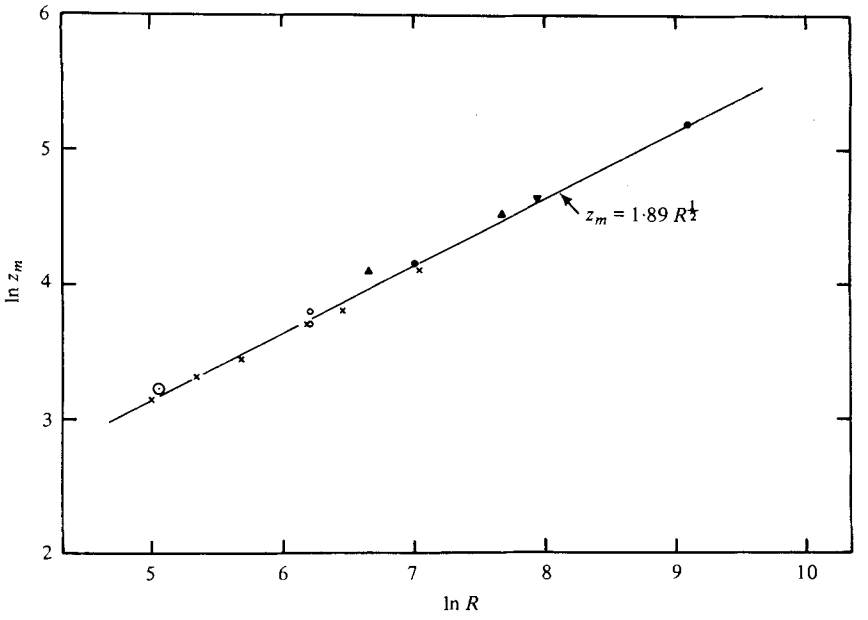

FIGURE 2. Distance z_m of maximum of Reynolds stress from wall for pipes and boundary layers. The line is $z_m = 1{\cdot}89R^{\frac{1}{2}}$, where $R = u_\tau a/\nu$ for a pipe and $u_\tau \delta_d/\nu$ for a boundary layer where δ_d is boundary-layer thickness. ×, Nikuradse, pipe; ●, Laufer, pipe; ⊙, Ueda & Mizushina, pipe; ▲, Gupta & Kaplan, boundary layer; ▼, Klebanoff, boundary layer; ○, Schildknecht *et al.*, boundary layer.

where $S = z\overline{u}_z$ and we use the exact equation (Monin & Yaglom 1971, p. 269)

$$T = 1 - zR^{-1} - \overline{u}_z. \tag{5}$$

Let us now consider the essential nature of the classical assumptions. One assumes that there is a region M_c far above the sublayer but far also from the centre of the pipe in which for large R mean quantities such as T_d are independent of ν and H as $\nu \to 0$ and $H \to \infty$. As we move in M_c toward larger and larger z_d, we experience ultimately a small but sensible and growing importance of H. *This should be felt first at some z_d of order H* or $z \sim R$, because ν is unimportant in the region M_c and further out. We see from (4), however, that the first effects of H (or R) are felt when the zR^{-1} term begins to compete with the z^{-1} term and that this occurs at $z \sim R^{\frac{1}{2}}$ (which is also the observed location of the maximum of T_d or T) and we find a *basic contradiction in the classical arguments.*† Evidently, the effects of viscosity are non-negligible in the transition region as our present theory reveals. Furthermore, (4) shows that the first effects of H or R for the curvature, T_{zz}, are felt in a different region, $z \sim R$, and that the order of T_{zz} is $R^{-\frac{3}{2}}$ in the transition region for T, $z \sim R^{\frac{1}{2}}$. In dimensional terms this means that the curvature of the Reynolds stress profile is proportional to $\nu^{-\frac{1}{2}}$ in a region (just before the transition of T to outer behaviour) in which ν is supposed to be negligible!

If we associate the maximum of the Reynolds stress with the transition region from inner to outer behaviour (and this seems to be a quite reasonable association), the true picture appears to be that of figure 3. Here the region of overlap is replaced by a transition region in the vicinity of $z \sim R^{\frac{1}{2}}$. In the new transition region both H

† In this connection, see the final paragraph of §5.

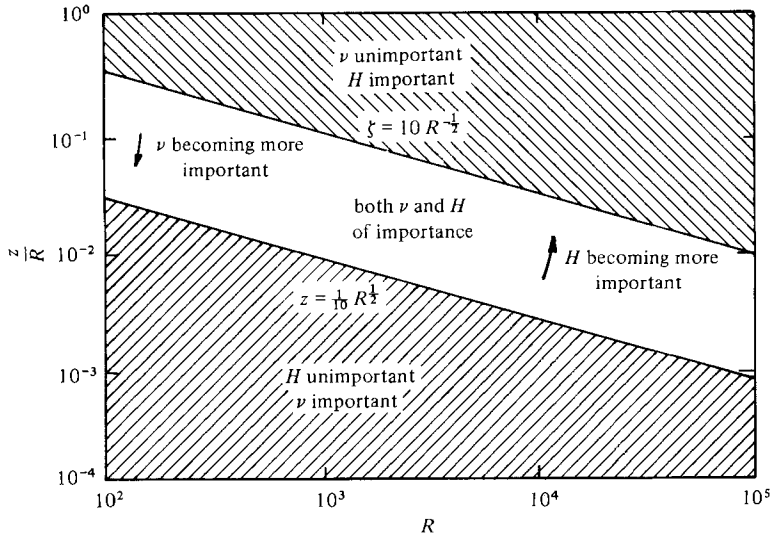

FIGURE 3. Inner, outer and transition regions in shear flow according to mesolayer theory. Symbols are explained in figure 1.

and ν are important although ν increases in importance as z decreases and H increases in importance as z increases. Because $1 \ll R^{\frac{1}{2}} \ll R$, *the transition region, which we call the mesolayer, intrudes between the inner and outer regions no matter how large the Reynolds number and prevents the overlap of classical theory.*

Physical insight into the nature of the mesolayer may be gained from recent theoretical and experimental studies of the distortion of turbulence in a wind tunnel by a surface parallel to the flow and adjusted to move at the speed of the free stream (Uzkan & Reynolds 1967; Thomas & Hancock 1977). The large eddies of length l are unaffected by the surface at distances $z_d > l$ but nearer to the surface they are distorted and the streamwise r.m.s. velocity increases at the expense of the normal r.m.s. velocity, reaching a maximum at a level $z_d \sim \delta_{dm}$ and then decreasing at distances $z_d < \delta_{dm}$ obviously because of friction. The thickness of this viscous boundary layer was measured to be $\delta_{dm} \cong 1{\cdot}8(\nu x_d/U_d)^{\frac{1}{2}}$, where x_d is the distance from the leading edge and U_d is the free-stream velocity. This relationship is derived by Hunt & Graham (1978) from the form assumed by the equations under the requirement that the vorticity of the free stream remains unchanged as the fluid moves over the region of the plate. Their theoretical constant of proportionality for the viscous layer thickness is quite different, however, from that of Uzkan & Reynolds and, moreover, their other theoretical results have only a fair agreement with observations. We therefore offer an alternative explanation for the thickness of the boundary layer which is also more relevant to our present purposes. To do this we first refer to a derivation by the first author (Long 1978*a*, *b*) of an energy source on an infinite plane, say at $x_d = 0$. The motivation for this was the construction of a theoretical model of turbulence in the vicinity of an oscillating grid (Thompson & Turner 1975; Hopfinger & Toly 1976). The energy source is characterized by a single constant K with the dimensions of viscosity. Dimensional analysis then gives the behaviour

$$\sigma_d \sim K/x_d, \quad l \sim x_d, \tag{6}$$

where σ_d is an r.m.s. velocity and l is the integral length scale. A model of turbulence in a wind tunnel may be constructed by passing a current of speed U_d along the x_d direction through the plane energy source. The energy equation for high Reynolds numbers is then

$$A_1 U_d \frac{\partial \sigma_d^2}{\partial x_d} + EFD + \frac{\sigma_d^3}{l} = 0, \tag{7}$$

where A_1 is a universal constant and EFD is the energy-flux divergence. In the stationary case, $\sigma_d l$ is invariant along x_d and, since the current simply carries the turbulence along with it, this relationship should continue to hold. If we now make the assumption that the speed of the current $U_d \gg \sigma_d$, as in Hunt & Graham (1978), we may neglect the middle term in (7) and then, using $\sigma_d l \sim K$, obtain

$$A_2 U_d \frac{\partial \sigma_d^2}{\partial x_d} + \frac{\sigma_d^4}{K} = 0. \tag{8}$$

Solving (8), we get

$$\sigma_d \sim (U_d K / x_d)^{\frac{1}{2}}, \quad l \sim (K x_d / U_d)^{\frac{1}{2}}. \tag{9}$$

The empirical formula for the boundary-layer thickness then becomes

$$\delta_{dm} \sim (\nu l / \sigma_d)^{\frac{1}{2}}. \tag{10}$$

Notice that this result may be obtained theoretically by assuming a balance of viscous forces of order $\nu \sigma_d / \delta_{dm}^2$ and inertial forces of order σ_d^2 / l acting on the eddies as they 'slosh' back and forth over the surface. This layer has a thickness identical to that of the proposed mesolayer in shear flow, $\delta_{dm} \sim (\nu H / u_\tau)^{\frac{1}{2}}$, because the large-eddy dimension l may be replaced by the outer length and the friction velocity by σ_d. Thus, one interpretation of the mesolayer is that it is the viscous boundary layer over which the velocity of the large eddies 'sloshing' over the surface tends to zero. Notice also that the mesolayer thickness is proportional to Taylor's microscale for the outer region.

Another interpretation arises from an investigation of thermal convection over a hot surface.† Here the same argument holds and the mesolayer thickness is as in (10). Dimensional arguments yield $\sigma_d \sim (qH)^{\frac{1}{3}}$, $l \sim H$, where q is the buoyancy flux and H is the depth of the convection layer, so that we may write $\delta_{dm} \sim \nu^{\frac{1}{2}} H^{\frac{1}{3}} q^{-\frac{1}{6}}$. In convection, an important phenomenon is the rise of thermals from a hot surface. They move slowly vertically but are observed also to be carried rapidly along the horizontal by the large eddies of size H filling the bulk of the container. These eddies have a speed of order $(qH)^{\frac{1}{3}}$ and a time scale of order $t_e \sim H^{\frac{2}{3}} q^{-\frac{1}{3}}$ and so, if we assume that the thermals grow by molecular conduction with coefficient κ, they obtain a size $(\kappa t_e)^{\frac{1}{2}}$ over the life of a large eddy after which we can presume that they are carried into the main portions of the container and torn apart. This dimension, $\kappa^{\frac{1}{2}} H^{\frac{1}{6}} q^{-\frac{1}{6}}$, precisely equals the mesolayer thickness δ_{dm} if we ignore variations in the Prandtl number. The thermals transport most of the heat in a region well above the sublayer (in which the effects of molecular conduction are assumed by classical arguments to be confined), yet their growth is apparently influenced by molecular conduction and in this way molecular processes must have a fundamental effect on the distribution of mean

† Dr C. S. Chern has collaborated with R. R. L. in this aspect of the work, and in some of the work reported in § 4 of this paper.

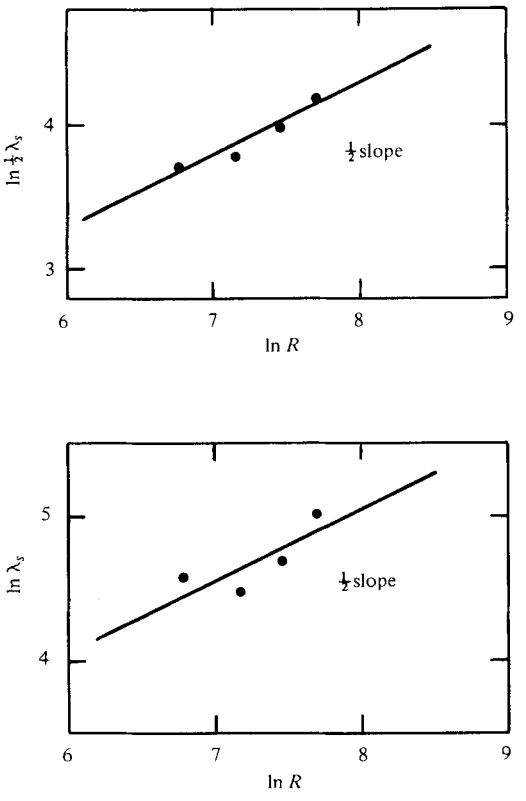

FIGURE 4. Streak-spacing according to Gupta, Laufer & Kaplan (1971). These are based on maxima and minima of correlations of streamwise velocity for variable spanwise separations. The two figures are for distance λ_s and half-distance $\frac{1}{2}\lambda_s$ between vortices. $\lambda_s = 2{\cdot}5R^{\frac{1}{2}}$, approximately.

quantities in a region far above the sublayer. In shear turbulence, observations indicate the existence of a 'burst' phenomenon, analogous, perhaps, to thermals, in which volumes of fluid also rise from the region of the sublayer and move upward and along the surface (e.g. Kline *et al.* 1967). If their surroundings are laminar, and this is frequently suggested by experimenters (e.g. Laufer 1975), they will grow after a time of the order of the outer eddy time H/u_τ to a size $(\nu H/u_\tau)^{\frac{1}{2}}$, which is again precisely the mesolayer thickness. These bursts are of great importance because they contain a considerable amount of the energy and account for much of the Reynolds stress (Nychas *et al.* 1973). Therefore, if we accept this physical picture it is not difficult to accept a certain role of molecular viscosity in a region well above the sublayer in conflict with the concepts of classical theory. Conversely, we may accept a role of the outer layer for conditions near the wall on the basis of observations that bursts originating near the wall have a statistically definable period that varies with the free-stream velocity and the outer layer thickness (Rao *et al.* 1971). The role of the outer layer near the wall has also been demonstrated by measurements (Tritton 1967; Mitchell & Hanratty 1966) that the integral length scale is very large, probably of the order of the outer length, as close to the wall as can be measured.

Thermals have been observed many times near a hot surface and appear simply as

blobs of hot fluid moving away from the wall. In the case of shear, however, the situation seems to be considerably different in that eddies with vorticity along the stream appear to occur in oppositely rotating pairs (Hinze 1975). They are revealed by the streaks of hydrogen bubbles which appear at the underlying surface and identify the line toward which the motions near the surface in the two vortices are directed. If these vortices, which appear to be the two legs of horseshoe or U-shaped vortices (Theodorsen 1955, 1962; Hinze 1975, p. 683) begin with very small radii they will grow by molecular diffusion of vorticity precisely to the mesolayer thickness in a time period of the order of that of the outer eddies. At the same time the interaction with the wall will produce a motion of the two vortices toward each other and, therefore, we expect them to be at a distance apart of the order of the mesolayer thickness too. If they are densely packed in the mesolayer, we also predict that the distance apart of the streaks observed at the wall should be proportional to the mesolayer thickness. This is contrary to the belief of experimentalists that the streaks are a distance apart of order $100\nu/u_\tau$ and therefore independent of the outer length. However, the available data (Gupta, Laufer & Kaplan 1971), although scanty and scattered, may, in fact, favour proportionality to the mesolayer thickness as we see in figure 4. Our present conjecture is that the flow, passing over the surface, generates an entire mesolayer packed with streamwise vortices and then an eddy comes along and sweeps this up into the fluid forming the 'backs' of the turbulent bulges in typical boundary-layer turbulence as revealed by the regions of warm fluid found there by Chen & Blackwelder (1978) in experiments with a passively heated plate. This region was found to be an internal shear layer containing fluid of low streamwise momentum, also suggesting an origin near the plate. One observer (Falco 1974, 1977, 1978), in fact, observed eddies in the turbulent boundary layer of dimensions of the order of Taylor's microscale for the outer flow which, we have noted, is also the mesolayer thickness.

4. The two components of motion in shear flow

According to our discussion and to the data, the presence of a mesolayer in the shear-free turbulence of Uzkan & Reynolds can scarcely be doubted. Because shear is also absent, we should strongly suspect the existence of the mesolayer in turbulent convection beneath the large eddies sloshing back and forth over the surface. We should expect, for example, that the r.m.s. tangential velocity profile would have a peak near the wall in the mesolayer. Such maxima in fact occur in experiments by Deardorff & Willis (1967) and more recently in experiments by Ferreira (1978) and Adrian & Ferreira (1979) as we see in figure 5. In Adrian & Ferreira we could compute the Reynolds number from the information in their paper. In Deardorff & Willis the measurements were made at three different Rayleigh numbers, $6{\cdot}3\times10^5$, $2{\cdot}5\times10^6$ and 10×10^6. We may estimate the corresponding values of the Reynolds number R by the following procedure: Using the empirical formula of Globe & Dropkin (1959), we obtain a Nusselt-number relation

$$Nu = 0{\cdot}069 Ra^{\frac{1}{3}} Pr^{0{\cdot}074},$$

where

$$R = (qH)^{\frac{1}{3}} H/\nu, \quad Nu = qH/\kappa\Delta b, \quad Ra = \Delta b H^3/\nu\kappa, \quad Pr = \nu/\kappa,$$

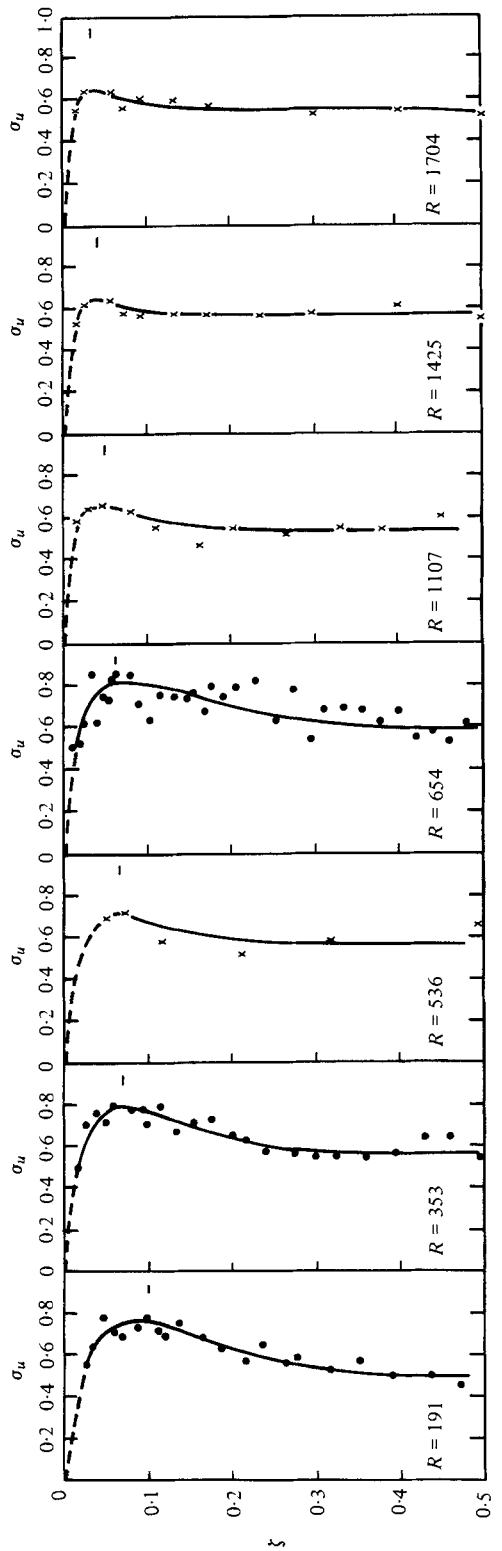

FIGURE 5. Profiles of tangential r.m.s. velocity in thermal convection. Deardorff & Willis (1967) had a hot and cold plate. In Ferreira (1978) and Adrian & Ferreira (1979) one plate was insulated.

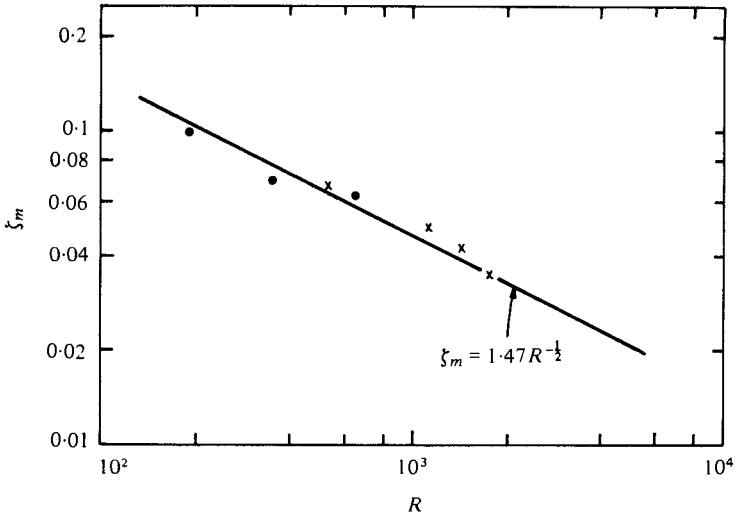

FIGURE 6. Location ζ_m of maximum of the tangential r.m.s. velocity profiles of figure 5. ×, Ferreira; ●, Deardorff & Willis.

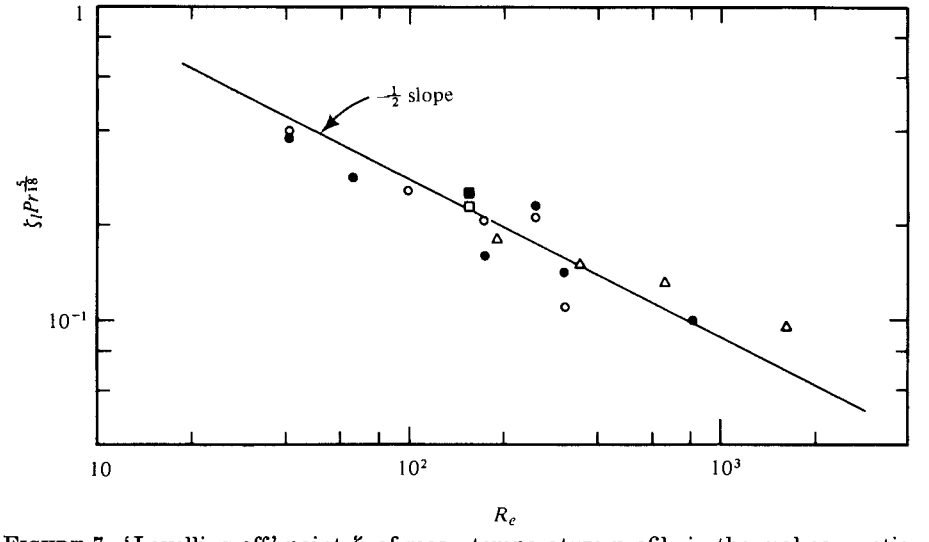

FIGURE 7. 'Levelling-off' point ζ_l of mean temperature profile in thermal convection in a plot appropriate for low Prandtl numbers. ○, Somerscales & Gazda (1969); △, Deardorff & Willis (1967); □, Thomas & Townsend (1957). Open symbols, hot plate; solid symbols, cold plate.

and Δb is the difference in buoyancy between the plates. Choosing $Pr = 0{\cdot}72$ for air, we estimate R to be 191, 353, 654, respectively, for the three Rayleigh numbers. If we use ζ as the distance from the wall scaled on the distance between the plates H, the locations of the maxima ζ_m in the two experiments are shown in figure 6 plotted against R. The agreement with the curve $\zeta_m = 1{\cdot}47R^{-\frac{1}{2}}$ is good and supports our theoretical determination of the mesolayer thickness in thermal convection. Another feature of turbulent convection between a lower hot surface and an upper cold surface which apparently brings out the role of the mesolayer is the behaviour of the mean

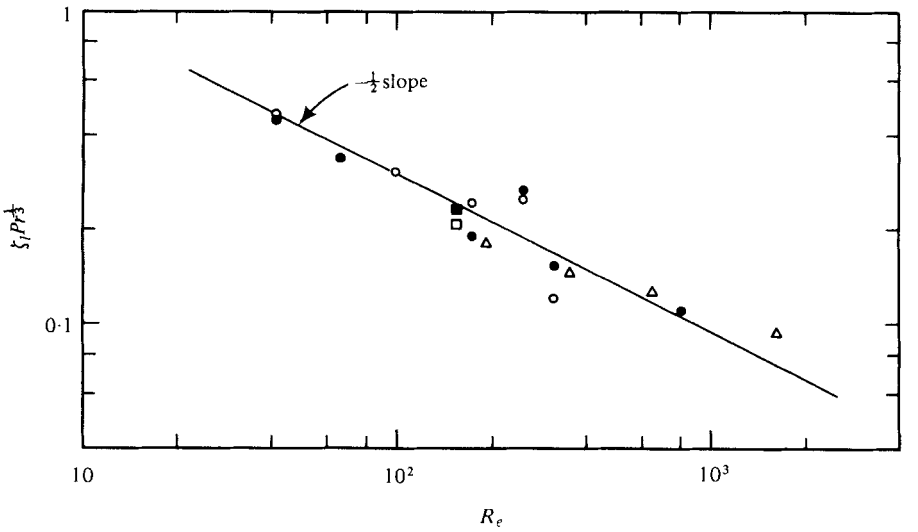

FIGURE 8. 'Levelling-off' point ζ_l of mean temperature profile in thermal convection in a plot appropriate for high Prandtl numbers. Key to data same as in figure 7.

temperature profile. In general the temperature decreases rapidly just above the hot surface and becomes isothermal in the interior region, decreasing rapidly again at the upper cold plate. This is modified somewhat at lower Rayleigh numbers where the interior temperature gradient actually reverses and one finds a level of minimum temperature at a certain height above the hot plate and a level of maximum temperature just below the cold plate. This gradient reversal is caused, evidently, by the large eddies bringing the cold or hot fluid from the upper or lower regions and so we would expect these extrema to be located in the mesolayer or, when the extrema are too weak to measure, that the levelling-off point, $\zeta = \zeta_l$, say, should be located in the mesolayer. In figures 7 and 8 we plot all available data on the 'levelling-off' point as $\zeta_l Pr^{\frac{5}{18}}$ and $\zeta_l Pr^{\frac{1}{3}}$ *vs.* the Reynolds number and we see that either choice causes a collapse of the data (corresponding to a Prandtl number range from 0·72 to 20) along lines of slope of $-\frac{1}{2}$ indicating that the point is fixed in the mesolayer or $\zeta_l \sim R^{-\frac{1}{2}}$. In a plot of ζ_l *vs.* R the collapse along a single line does not occur obviously because of the Prandtl number dependence. There are two problems in this regard: The theory gives a Nusselt number/Rayleigh number relationship $Nu \sim Ra^{\frac{1}{3}}$ for large Rayleigh numbers but the 'constant' is an unknown function of Pr. In Long (1976), the Prandtl number dependence is derived for high and low Pr but this older theory is based on classical matching procedures and must be replaced by the mesolayer approach. We have not done this but it appears that the results are the same, namely

$$Nu \sim Ra^{\frac{1}{3}} Pr^{\frac{1}{3}} \quad (\text{low } Pr), \tag{11}$$

$$Nu \sim Ra^{\frac{1}{3}} \quad (\text{high } Pr). \tag{12}$$

The second difficulty is that the theory assumes a fixed Prandtl number and so the dependence of the mesolayer thickness on Pr is also unknown. We can overcome one of these difficulties by using the finding that there is a collapse of the data for a plot of ζ_l along a curve $Ra^{-\frac{2}{5}}$. With this and the two behaviours in (11) and (12) we obtain

the factors of ζ_l in figures 7 and 8. Of course there is very little difference between these powers of Pr and we certainly cannot make a choice but the important fact remains that the 'levelling-off' point is at $R^{-\frac{1}{2}}$ at any given Prandtl number.

According to classical ideas of shear flow over a surface and also of thermal convection, the eddies near the surface have velocities of the order of the friction velocity u_τ in shear flow or $(qz_d)^{\frac{1}{3}}$ in convection and dimensions l_+ of order of the distance from the surface. The argument is that as one moves upward the viscous terms, proportional to l_+^{-2}, decrease faster than the inertial terms, proportional to l_+^{-1}, and viscosity becomes negligible above a height of order ν/u_τ in shear flow, say, above $z_{di} = a_i \nu/u_\tau$, where a_i is a constant. In the interior viscosity is unimportant and quantities vary with u_τ and the outer length H; for example, the typical eddy has a velocity of order u_τ and dimensions of order H. Moving downward, the eddies diminish in size and eventually below the level $z_{d0} = a_0 H$ all length scales except those of the fine structure become controlled by distance from the surface. The two points z_{di} and z_{d0} become more and more separated in physical space as the Reynolds number becomes large and the region between these points becomes the classical region of overlap.

It is reasonably clear how this picture must be changed to accommodate a mesolayer. We recognize that the large eddies whose sloshing creates the mesolayer have dimensions characteristic of the outer length and that such eddies would be absent if the outer length were infinite. This suggests that we should regard the turbulence as having two components, as indeed has been suggested by several authors in recent years, for example Townsend (1976, p. 161). Townsend calls the large eddies the 'inactive' component of turbulence; the others constitute the 'wall' component. The large eddies are such an important part of the problem in the theory of the present paper that the word 'inactive' seems inappropriate and we prefer the description of Perry & Abell (1977) who call the two components 'universal' and 'nonuniversal'. As suggested by the name, the universal component has linear dimensions which all scale on distance from the wall as in the classical picture. The non-universal components reflect the existence of the large outer eddies. The two components of motion appear clearly in spectra at high Reynolds numbers (Perry & Abell 1975; Bullock, Cooper & Abernathy 1978).

We obtained the thickness of the viscous layer in shear-free turbulence by equating the orders of the viscous and inertial terms. Shear turbulence is more involved because there is already one viscous layer (sublayer) at the wall in a pipe or boundary layer and it is not immediately obvious how to obtain another one from a single set of Navier–Stokes equations. We can do it, however, if we break up the motion into the two components, for example

$$u = u_+ + u_*, \quad \overline{u} = \overline{u}_+ + \overline{u}_*, \tag{13), (14}$$

where u is the instantaneous velocity in the turbulent flow. The terms with the plus suffix correspond to the universal component and the terms with the star suffix to the non-universal component. Only the first component survives when the outer length goes to infinity, and so it satisfies the Navier–Stokes equations by itself for all R. We call this set of equations N_+. This may then be subtracted from the full set N to yield a new set of equations N_*, valid at finite R. The N_* equations are complicated because of the nonlinearity of the inertia terms, but the viscous terms are derivatives of the second component only. It may be shown that by integrating over a 'box' in

the mesolayer the small-scale effects in the inertial terms of N_* can be eliminated. In the case of pipe flow this yields R^{-1} for the order of the inertial terms and δ_m^{-2} for the order of the viscous terms, where δ_m is the non-dimensional thickness of the boundary layer. Thus $\delta_m \sim R^{\frac{1}{2}}$ and we obtain the second viscous boundary layer (mesolayer) in much the same way as in shear-free turbulence.

The importance of friction on the non-universal component

We have mentioned that the mesolayer thickness is proportional to Taylor's microscale and we find this significant, but the current viewpoint in turbulence appears to be that the Taylor microscale has mathematical but not physical significance. We may explain the importance of friction at distances so far above the sublayer by referring again to (3). This shows that near the wall ($z \ll R$), the sum of the viscous and Reynolds stresses is nearly constant. Since the viscous term is extremely small except in the sublayer, it decreases rapidly in this layer and above, and T rapidly approaches 1. We deduce, first, the classical result that the sublayer is the region $z \sim 1$ in which Reynolds *stresses* and viscous *stresses* are of the same order. Further up in the fluid in the region where T is nearly constant, the term z/R in (3) must ultimately begin to have importance. If we differentiate (3) we obtain

$$\frac{1}{R} = \frac{\partial T}{\partial z} + \frac{\partial^2 \bar{u}}{\partial z^2} \tag{15}$$

and this shows that the *force* due to the Reynolds stress is small, of order R^{-1}, so that *viscous forces are not negligible despite their smallness*. In summary, frictional forces in the mesolayer are very weak, to be sure, because the thickness of the mesolayer is much greater than the sublayer, but the inertial forces obtained by differentiating a very nearly constant Reynolds stress are also very small and neither can be neglected. The balance of these two small forces, of course, defines the thickness of the mesolayer. The viscous forces on the first component of motion are negligible in the mesolayer because the inertial forces on this component are large, but the viscous forces acting on the second component are not negligible because the enormous horizontal length scale of the second component $l \sim H$ means weak inertial forces and therefore *comparatively* important viscous effects. Figure 9 summarizes the discussion.

A rather similar situation exists in wavenumber space. Investigation of the spectrum arises from the conjecture that the layer in physical space of thickness of order of Taylor's microscale should have a counterpart in wavenumber space corresponding to eddies of the size of Taylor's microscale. We may show most simply that a region of this kind exists for a turbulence model of the author (Long 1978*a*) for the decay of homogeneous turbulence following a distribution in space at $t = 0$ of singularities used to develop the energy source on a plane (Long 1978*b*). One obtains

$$\sigma_d \sim (K/t)^{\frac{1}{2}}, \quad l \sim (Kt)^{\frac{1}{2}}, \quad \epsilon_d \sim K/t^2, \tag{16}$$

where the constant K with dimensions L^2T^{-1} is again characteristic of the energy source at all points of space at the initial instant $t = 0$. This is a special case of self-preserving turbulence (Korneyev & Sedov 1976). The Reynolds number is a constant $R = K/\nu$ and (16) assumes large R. We also need the energy equation (Hinze 1975, p. 215)

$$\partial E/\partial t = F - D, \tag{17}$$

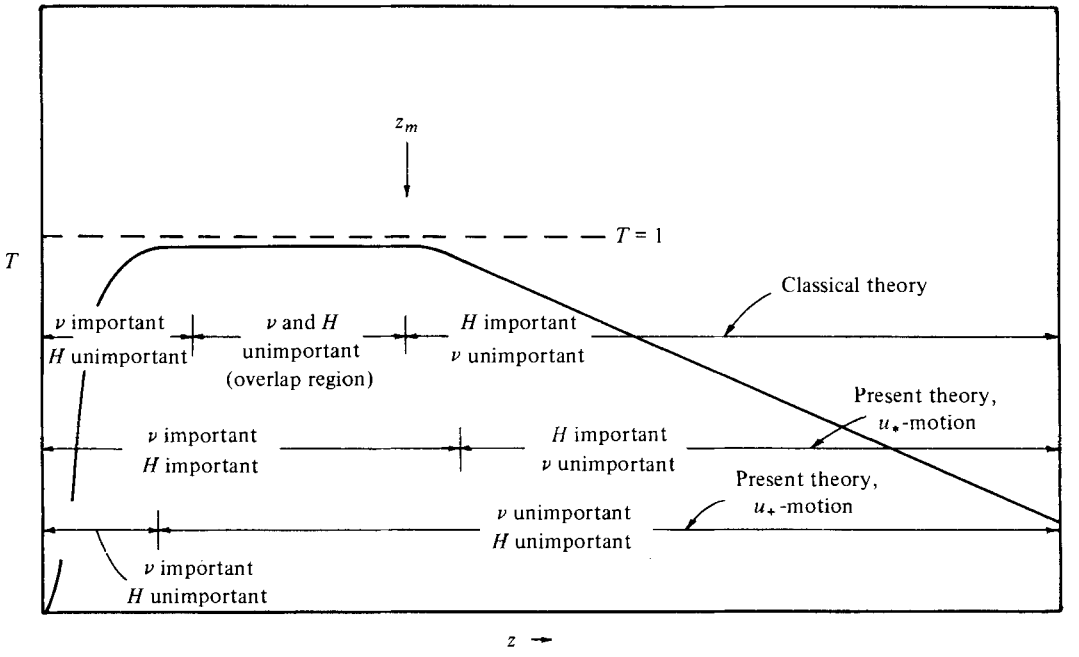

FIGURE 9. Various regions in shear flow in a pipe, according to classical theory and present theory. The curve is a schematic picture of the Reynolds stress.

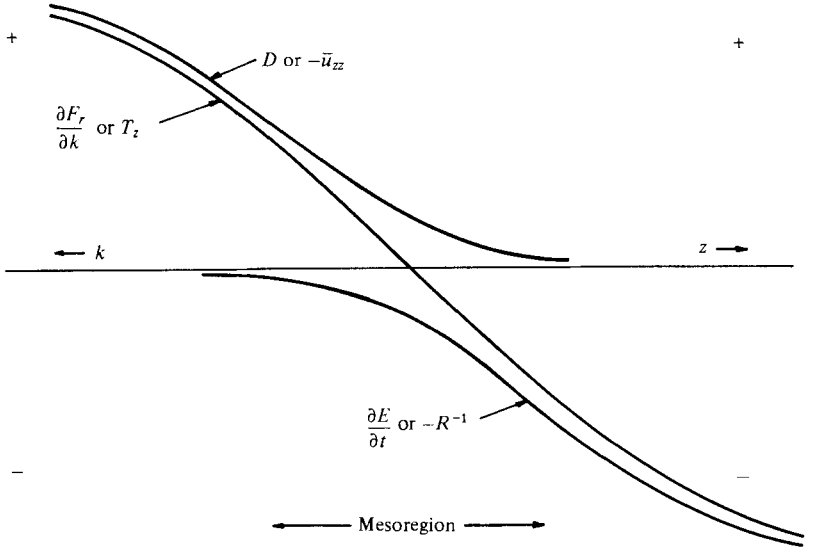

FIGURE 10. Schematic behaviour of terms in the energy equation for the spectrum and the momentum equation for turbulence in pipe flow. Refer to (15) and (17).

where $F = \partial F_r/\partial k$ is the energy transfer from smaller to larger wavenumbers and $D = 2\nu k^2 E$ is the viscous dissipation. In the inertial range, $k \sim k_e \sim l^{-1}$, we assume that $E \sim \epsilon_d^{\frac{2}{3}} k_e^{-\frac{5}{3}}$ and in viscous range $k \sim k_d$ that $E \sim \epsilon_d \nu^{-1} k_d^{-3}$, where k_d is the inverse of the Kolmogorov scale η. We see then that $(\partial E/\partial t)/D$ is of order R in the inertial range and of order $R^{-\frac{1}{2}}$ in the viscous range. The situation is portrayed schematically

in figure 10. At smaller wavenumbers, the time-rate-of-change (decrease) of energy is close to the nonlinear transfer (loss) of energy and dissipation is small. At larger wavenumbers the time-rate-of-change (loss) of energy is small and nonlinear transfer (gain) of energy is closely balanced by viscous dissipation. Obviously since F changes sign and so is zero at an intermediate wavenumber, $\partial E/\partial t$ and D are of the same order in a range of wavenumbers $k_m \sim (\nu t)^{-\frac{1}{2}} \sim \lambda^{-1}$ and we find the mesoregion in wavenumber space.

There is a certain analogy between the energy equation in (17) and the momentum equation in (15) and we illustrate this in figure 10. The viscous force is directly analogous to the dissipation term; the Reynolds stress force is analogous to the nonlinear transfer F and the term R^{-1} is analogous to $\partial E/\partial t$. In other problems the term on the left-hand side of (15) will be more complicated; for example, it is equal to the imbalance of Coriolis force and pressure gradient force in the direction transverse to the surface stress in the problem of the neutral Ekman layer (§ 7). In the spectrum, the vicinity of Taylor's microscale in wavenumber space is a region where the dissipation D is very small, to be sure, but here the nonlinear transfer of energy from one wavenumber to another, F_r, is a maximum and so its derivative F in (17) is very small too. We conclude that we can no more neglect friction for $k \sim \lambda^{-1}$ than we can neglect the inertial effects of the nonlinear transfer term in the region. The significance of the mesoregion for the spectrum is akin to that in shear flow in that a matching of the inner ($k \sim k_d$) and outer ($k \sim k_e$) regions to derive the classical $k^{-\frac{5}{3}}$ behaviour for E is not possible because of the intruding mesoregion.

5. Turbulent flow in a pipe

If we accept the existence of the mesolayer (on the basis of the arguments and evidence in this paper), the problem is then to so change the approach of classical theory, which leads to the logarithmic boundary layer in shear flow, for example, as to include the contribution of the mesolayer. We have done this in the cases mentioned in § 1. Putting the mesolayer into a new theory seems at first glance to be rather simple in that we need only construct a new law of the wall incorporating the mesolayer and then match the mean expressions in this larger, inner region with the mean expressions in the outer region wherein we impose Reynolds number similarity. A different set of problems arises in each application, however, and we cannot give many of the details here. But the basic approach may be illustrated quite simply by the example of pipe flow. The classical approach assumes first an inner region near the wall of the pipe in which the mean velocity may be expressed as in (1)

$$\overline{u} = u_+(z), \quad z = z_d u_\tau/\nu,$$

where we scale as usual on the friction velocity at the wall u_τ and viscosity ν and where z_d is distance from the wall. Secondly, the classical theory assumes that the velocity defect in the outer region may be expressed as

$$U - \overline{u} = u_0(\zeta), \quad \zeta = z/R, \quad R = u_\tau a/\nu, \tag{18}$$

where $U = U_d/u_\tau$ (U_d is the velocity at the centre-line) and R is the Reynolds number scaled on the radius of the pipe a. Finally, the assumption of the overlap yields the classical logarithmic behaviour of the mean velocity in the overlap region by arguments

first given by Izakson (1937) and Millikan (1938). One obtains as a bonus the logarithmic drag law (Monin & Yaglom 1971). In mesolayer theory a new layer $z \sim R^{\frac{1}{2}}$ intrudes between the inner and outer layers and must be taken into account. We do this by defining a new similarity variable $\hat{z} = z/R^{\frac{1}{2}}$ and represent the contribution of the mesolayer to first order by adding the product of a function of $\hat{z}$ and a function of R to the right-hand side of (1), i.e.

$$\overline{u} = u_+(z) + h(R)\, u_*(\hat{z}), \tag{19}$$

where $h(R)$ is to be determined. The first term in (19) is now the contribution of the universal component of the turbulent motion and therefore does not involve the outer length, i.e. the Reynolds number. Physically, it is the mean velocity over an infinite flat plate in infinite half-space for the given finite value u_τ of the friction velocity at the surface. The function $h(R)$ follows from the mean momentum equation. Thus, we expand the Reynolds stress in the same fashion

$$T = T_+(z) + g(R)\, T_*(\hat{z}), \tag{20}$$

and then substitute (19) and (20) into the momentum equation which is the derivative of (3). We obtain

$$u_+'' + T_+' = 0, \quad R^{-1}hu_*'' + R^{-\frac{1}{2}}gT_*' = -R^{-1}, \tag{21}$$

where the first equation follows by letting $R \to \infty$ at fixed z. Equation (21) shows clearly that $h = 1$ and $g = R^{-\frac{1}{2}}$. The matching condition becomes

$$U - \overline{u} = u_0(\zeta) = U(R) - u_+(z) - u_*(\hat{z}). \tag{22}$$

We may now proceed mathematically with one additional requirement that the flow in infinite half-space be independent of ν at large z_d. We get

$$u_+ = S_{00}^+ \ln z + C_{00}^+ \quad (z \gg 1), \tag{23}$$

$$U = A_{00} + C_{00}^+ + C_{00} + (S_{00}^+ + \tfrac{1}{2}S_{00}^*) \ln R \quad (R \gg 1), \tag{24}$$

$$u_* = S_{00}^* \ln \hat{z} + C_{00} \quad (R^{\frac{1}{2}} \ll z \ll R), \tag{25}$$

$$U - \overline{u} = A_{00} - (S_{00}^+ + S_{00}^*) \ln \zeta \quad (R^{\frac{1}{2}} \ll z \ll R), \tag{26}$$

where $S_{00}^+, C_{00}^+, S_{00}^*, \ldots$ are universal constants. The expressions for the velocity in (23) and (26) are similar to those of classical theory but the two regions are different. We also obtain the same drag law, to first order, as in classical theory. In (23) the expression for the inner form of the mean profile will approximate the mean velocity in a region $1 \ll z \ll R^{\frac{1}{2}}$ above the sublayer and below the centre of the mesolayer. Additional arguments permit passage to higher approximations and so to infinite series for the drag law and mean quantities in $1 \ll z \ll R^{\frac{1}{2}}$ and $R^{\frac{1}{2}} \ll z \ll R$.

Experiments indicate that S_{00}^+ in (23) is close to κ^{-1}, where κ is von Kármán's constant, and that S_{00}^* is rather small. This means that the mesolayer does not show up strongly with respect to mean velocity; indeed in the beginning of the investigation on pipe flow there did not appear to be any obvious way to use the mean velocity profile to illustrate the existence and importance of the mesolayer. But we will see shortly that closer inspection reveals a systematic departure of the mean velocity profile from the single logarithmic curve of classical theory and the mesolayer can be identified.

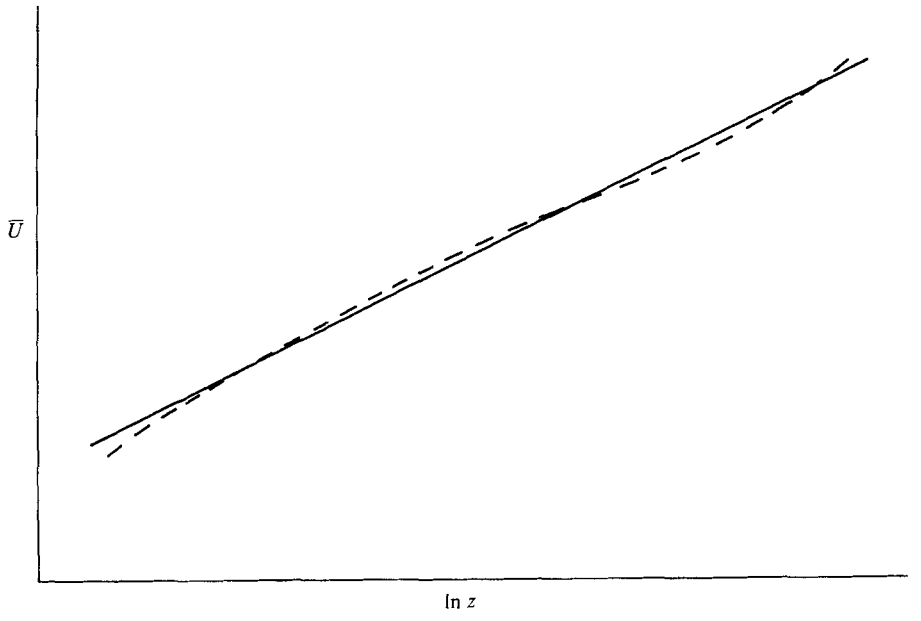

FIGURE 11. Schematic variation of mean velocity profile in pipe flow.

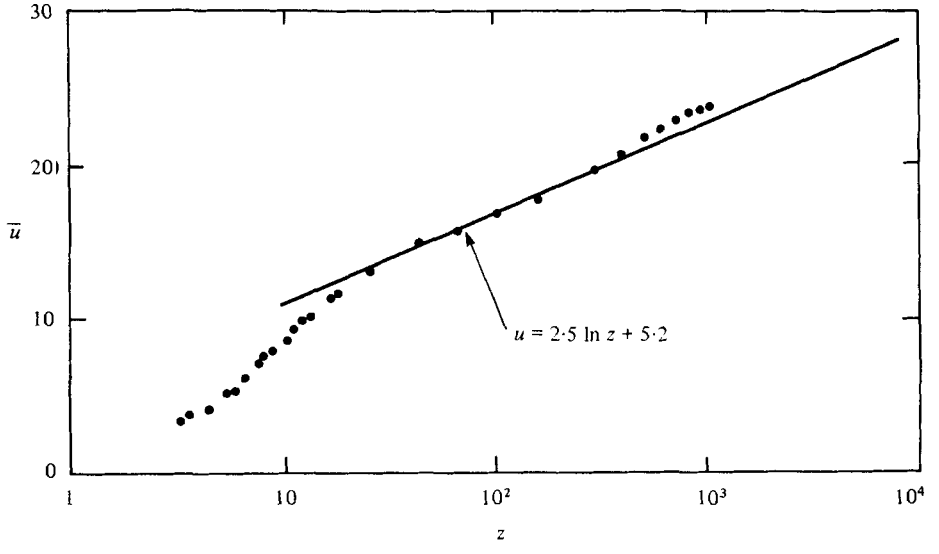

FIGURE 12. Mean velocity profile in a pipe (Laufer 1954). $R = 1150\ (= u_\tau \alpha/\nu)$.

Additional terms from higher approximations permit a qualitative picture of the behaviour of the mean velocity in the vicinity of the mesolayer, as shown in figure 11. One's first reaction to the data on mean velocity in a pipe, for example that by Laufer (1954) and Perry & Abell (1975), is that within the accuracy of the measurements the trend in a thick layer between $z = 1$ and $z = R$ is along a logarithmic curve with a slope given by von Kármán's constant. This is a surface impression, however, resulting

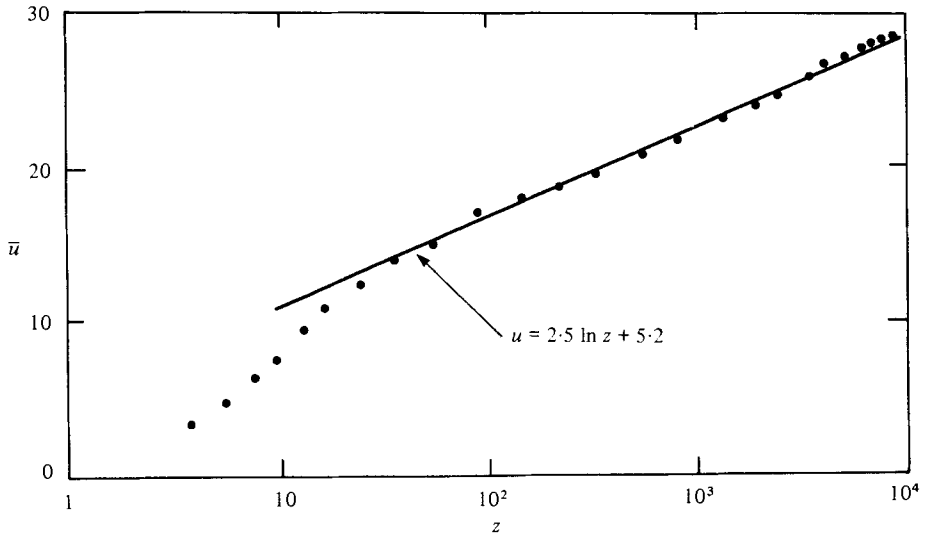

FIGURE 13. Mean velocity profile in a pipe (Laufer 1954). $R = 8750$.

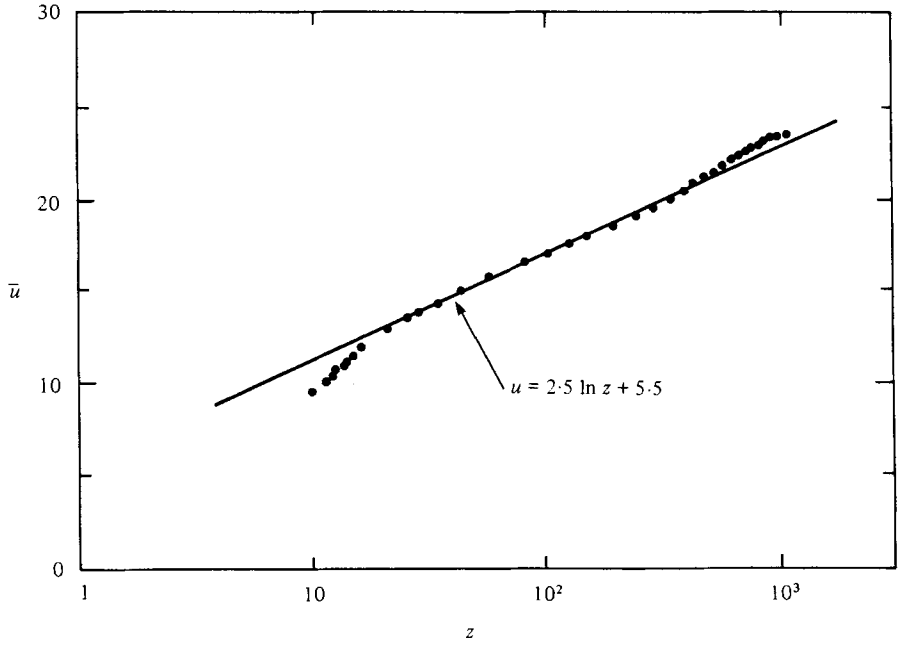

FIGURE 14. Mean velocity profile in a pipe (Hishida & Nagano 1979). $R = 905$.

from the practice of plotting measurements of mean velocity for many Reynolds numbers on the same figure. The resulting confusion is illustrated in figure 3 of the paper by Perry & Abell (1975). Even in the absence of data at a particular Reynolds number, it is obvious that the weak variation about the straight line of figure 11 will be obscured when experiments over a range of Reynolds numbers are plotted together if, as is the case, the location of the transition from one logarithmic behaviour to another varies with R. But individual cases are enlightening. We show examples

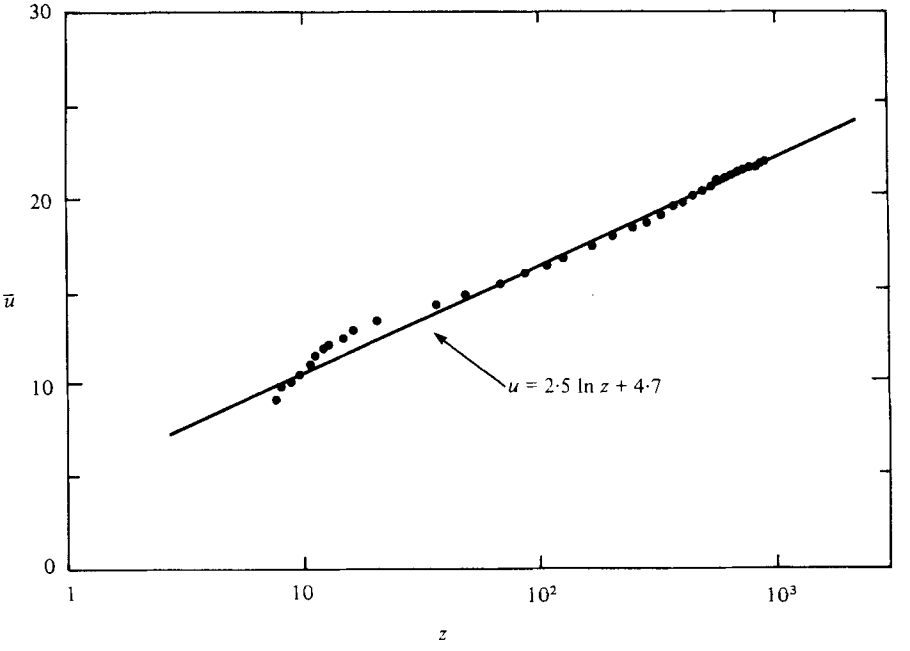

FIGURE 15. Mean velocity profile in a pipe (Hishida & Nagano 1977). $R = 905$. The pipe walls are slightly heated in this case.

in figures 12–15 of mean velocity profiles in a pipe for four Reynolds numbers. Figure 15 is for the same Reynolds number as figure 14 but the pipe is slightly heated. The predicted behaviour of figure 11 is revealed in each of these experiments although rather weakly in some cases. Most importantly, however, the transition region quite obviously varies with the Reynolds number as we see by comparing figures 12 and 13 in which the Reynolds numbers differ considerably. We notice that the transition region (mesolayer) moves outward roughly in accordance with the theoretical $R^{\frac{1}{2}}$ behaviour, but data below the mesolayer do not exist in most pipe experiments (e.g. those of Nikuradse 1932) and we could not verify the $R^{\frac{1}{2}}$ behaviour quantitatively. We were able to do just this for a boundary layer and we give results in the next section.

We present additional evidence for the existence of the mesolayer in pipe flow from the measured profiles of the streamwise r.m.s. velocity σ_u. Observations indicate that the curve rises sharply from the wall to a maximum located at $z \sim 1$ and then decreases. The classical theory, however, predicts that it should become constant and we portray this in the curve labelled σ_{u+} in figure 16. Perry & Abell (1975) believe, as do we, that the curve drops because of the influence of the outer region (outer length R) and that the region of constancy is unclear in the data because of the modest Reynolds numbers of the experiments. The data in their figure 7 show a region around $z = 100$ where σ_u appears to level off at higher Reynolds numbers and they believe that this is the classical overlap region. At the highest Reynolds number, however, there is a weak tendency for σ_u to actually increase again to a secondary maximum in the manner of the dashed curve in figure 16 and classical theory does not explain this. In mesolayer theory, σ_{u+} should also have the classical behaviour of figure 16, and the secondary maximum is explained by the tendency of the outer eddies to cause

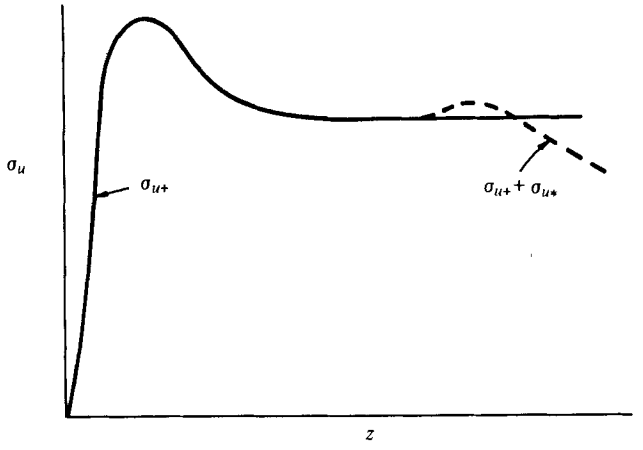

FIGURE 16. Schematic behaviour of σ_u profiles. $\sigma_u = \sigma_{u+} + \sigma_{u*}$.

another maximum of σ_u in the mesolayer as in shear-free turbulence (Uzkan & Reynolds 1967; Thomas & Hancock 1977) and thermal convection (Willis & Deardorff 1967; Adrian & Ferreira 1979; our figure 5). In shear flow we should not be surprised that this tendency is weakened by the influence of the outer length causing σ_u to decrease.

The outer eddies have a velocity scale u_τ and they create the second component in the mesolayer. Therefore the second component of motion is of first-order importance and so the first two terms in the mesolayer expansion for σ_u should be

$$\sigma_u = \sigma_{u+}(z) + \sigma_{u*}(\hat{z}). \tag{27}$$

In the mesolayer where $z \gg 1$, σ_{u+} will have its asymptotic, constant value and so the curves of σ_u should collapse in at least a thin region for all Reynolds numbers when plotted against the similarity variable $\hat{z}$ rather than z. The plot of the data of Perry & Abell in figure 17 shows that the region of collapse exists and is centred at $\hat{z} = 4{\cdot}0$, approximately. The behaviour of σ_u in a pipe which encouraged Perry & Abell in their efforts to verify classical theory also encourages us in our efforts to verify mesolayer theory and this illustrates the frequent difficulties in our earliest efforts to distinguish mesolayer theory from classical theory even though they are different in principle and give predictions which are different in appearance at high enough Reynolds numbers.

The r.m.s. normal velocity is little influenced near the wall by the second component of motion because $\sigma_{w+} \sim 1$ but, from continuity, $\sigma_{w*} \sim R^{-\frac{1}{2}}$. This explains the relative deepness of the layer of the law of the wall for σ_w as mentioned in § 2.

The constant S^*_{00} in (24)–(26) must be small and negative,† because the velocity profiles in a logarithmic plot has a smaller slope above the mesolayer than below. This means that the contribution of the second component of turbulent motion to

† The first determination of Kármán's constant was $\kappa = 0{\cdot}41$ by Nikuradse who had no data in the inner portions of the mesolayer. Then, we may reasonably take $S^+_{00} + S^*_{00} \cong 2{\cdot}37$. We cannot make a very good estimate of S^+_{00} but it appears to be, perhaps, 2·89. If we define $(S^+_{00})^{-1}$ as the 'proper' von Kármán's constant we have a new estimate 0·35 close to that measured by Businger *et al.* (1971) in the atmosphere. Then $S^*_{00} \cong -0{\cdot}52$.

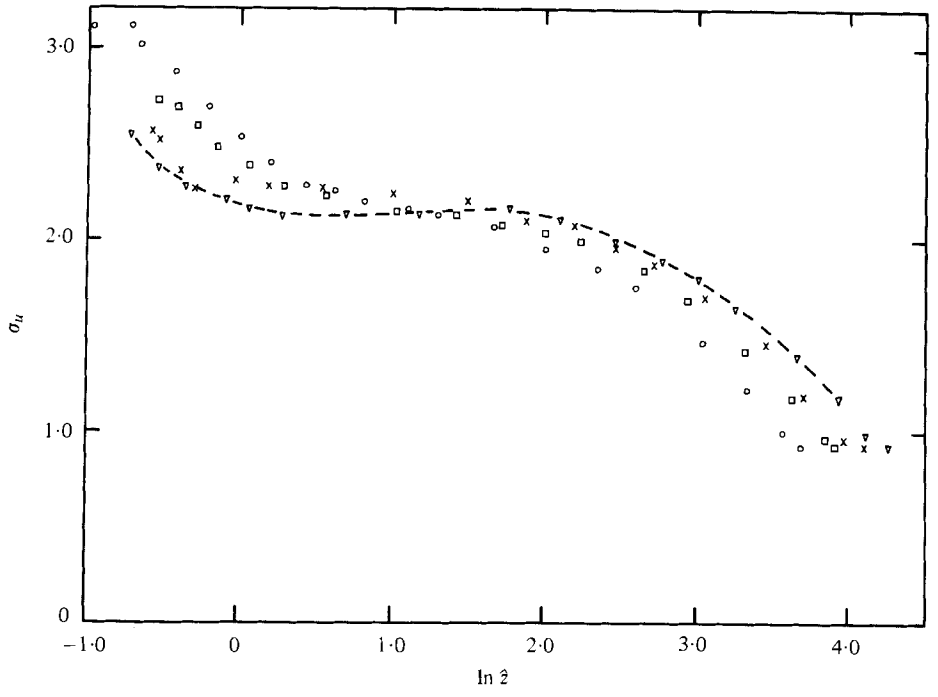

FIGURE 17. Profiles of r.m.s. streamwise velocity in a pipe against $\hat{z}$ (Perry & Abell 1975). Reynolds numbers: ○, 1603; □, 2607; ×, 3313; ▽, 4755.

the mean velocity, $\overline{u}_*$, is negative in the outer part of the mesolayer, as indeed it must be in most of the outer region because observations show that the mean velocity in the centre of the pipe is *less* than that given by the component in (23). Moreover, according to (25), $\overline{u}_*$ decreases outward (C_{00} may be small negative). We would expect, therefore, that the eddy flux of momentum due to the second component T_* should cause a transfer of momentum *outward*, i.e. in the opposite direction to T_+ but properly down the gradient of $\overline{u}_*$. Thus the gradual decrease of T beyond the centre of the mesolayer is attributable directly to the tendency for $\overline{u}_*$ momentum to flow toward the centre of the pipe. This may be regarded as a rough physical explanation why the maximum of T lies at $z \sim R^{\frac{1}{2}}$, i.e. in the mesolayer. We have said that the smallness of S_{00}^* means a weak (although order one) contribution of the second component to the mean velocity and thus to the observed smallness of the 'correction' (Hinze 1975, p. 721) to the logarithmic profile at the centre of the pipe. In a boundary layer this 'correction' is larger and we would then anticipate that the mesolayer effect would show up more strongly in a boundary layer than in a pipe. We will see that this is so in the next section.

We have assumed on the basis of the 'sloshing' argument of § 3 that a mesolayer of thickness $R^{\frac{1}{2}}$ exists. We may improve the discussion of this and see the vital importance of the mesolayer as follows: We may write the inner forms for the mean velocity and Reynolds stress as in (19) and (20) except now $\hat{z} = z/m$, where $m(R)$ is the undetermined thickness of the mesolayer. Of course we may recover classical theory by putting $h = 1$, $g = 1$, $m = 1$ or $u_* = T_* = 0$. Substituting (19) and (20) into (5) and letting $R \to \infty$, we get

$$u'_+ + T_+ = 1. \tag{28}$$

Subtracting (28) from (5) we have, also,

$$hm^{-1}u'_* + gT_* = -zR^{-1}. \tag{29}$$

Differentiation of (29) yields

$$hm^{-2}u''_* + gm^{-1}T'_* = -R^{-1}. \tag{30}$$

We now use the fundamental property of the mesolayer, $\hat{z} \sim 1$, that inertial and viscous forces for the second component are of the same order in the layer. Then in (30) $h = mg$. Using dimensional analysis and independence of ν for the first component in regions above the sublayer, u'_+ in (28) is proportional to z^{-1} in the mesolayer (or at any large z). Using (28)

$$u'_+ \to S_k^+ z^{-1}, \quad T_+ \to 1 - S_k^+ z^{-1},$$

where S_k^+ is a universal constant. Then, in the mesolayer, we have

$$T = 1 - S_k^+ z^{-1} m^{-1} + gT_*.$$

The Reynolds stress T is zero at the wall of the pipe and zero also at the centre of the pipe and so, as also observed, it is a maximum at some distance z_4 from the wall. Clearly, this cannot occur in the outer region because there is a vicinity of the maximum where the viscous and Reynolds stress forces are of the same order and this is the property of the mesolayer. Thus $z_4 = a_4 m$, where a_4 is a universal constant. We may also look at this as follows: $T'_+ = S_k^+ z^{-2}$ in the mesolayer (where $z \gg 1$) and this clearly dominates the slope of T at smaller z. The negative contribution to the slope from the second component of the turbulent motion, $gm^{-1}T'_*$ is negligible at smaller z and dominates at larger z since the slope must become negative at larger z. Thus

$$S_k^+ a_4^{-2} m^{-2} = -gm^{-1}T'_*(a_4), \tag{31}$$

and so $g(R) = m^{-1}$. From (5) $\overline{u}_{zz}(z_4) = -R^{-1}$ or

$$hm^{-2}u''_*(a_4) - (S_k^+ a_4^{-2} m^{-2} = R^{-1}. \tag{32}$$

This shows $h = 1$, $m = R^{\frac{1}{2}}$ and we obtain the mesolayer thickness again and the location of the maximum at $z_4 \sim R^{\frac{1}{2}}$ in agreement with the slope of the curve of figure 2. Of course, we may attempt to rescue classical theory by putting $u''_*(a_4) = 0$, but we have no theoretical or other reason for doing this. We establish at the very least that the present theory is competitive with classical theory. But we can do more: If we follow classical thinking and neglect the mesolayer contribution in (32) we get

$$a_4 = (S_k^+)^{\frac{1}{2}}.$$

Then using $a_4 = 1{\cdot}89$ from figure 2 we find $\kappa \cong 0{\cdot}28$ for von Kármán's constant, which is absurdly small. This is one of the most supportive pieces of evidence in this paper. The mesolayer simply has to be there to build up the needed deficit in the von Kármán constant. Furthermore, despite the uncertainty in our estimations of S_{00}^* and S_{00}^+ we can show good agreement with our estimation of the mesolayer contribution to the location of the maximum of the Reynolds stress and the mesolayer contribution to the mean velocity. The former is $0{\cdot}19/1{\cdot}70$ or 12 % and the latter is $0{\cdot}52/2{\cdot}89$ or 18 % of the contribution of the first component. There is no theoretical reason why these percentages need be the same because the maximum of the Reynolds stress is not necessarily in the outer portions of the mesolayer but the closeness of the two percentages is favourable to our ideas. We emphasize that the contributions of the

mesolayer in the two cases are numerically small *but of the same order of magnitude as the first (classical) component.* Perhaps, the main significance of the smallness is that it permitted the classical theory to survive for so long!

An argument against the mesolayer theory by one of the referees was that classical theory predicts the constancy of T in a region $1 \ll z \ll R$ and so, at best, mesolayer theory provides only a small correction to classical theory. Such an argument contains a slight appeal but can be advanced only because T is of order one and the mesolayer contribution is asymptotically small, of order $g \sim R^{-\frac{1}{2}} \ll 1$. The argument is quite wrong for most mean quantities including the mean velocity and the tangential r.m.s. velocities in a pipe and, more pertinently, for the slope of the curve of Reynolds stress. The present theory works for all of these *and* for T itself. The classical theory is wrong even with respect to order of magnitude for the mean velocity in the Ekman layer (§ 7).

6. The turbulent boundary layer at zero incidence

Let us now consider enough of the theory of a turbulent boundary layer to enable us to relate the large amount of experimental data to the new mesolayer theory. The theoretical model is flow with uniform velocity U_d along the x axis moving over a flat plate extending from $x_d = 0$ to $x_d = \infty$ as in figure 18. We assume that a turbulent layer develops over the plate of thickness $\delta_d(x_d)$ and that the stress at the surface is $u_\tau^2(x_d)$.

Variation of friction velocity with distance along the plate

Let us try a preliminary scaling, as in the classical approach, on the local friction velocity u_τ and viscosity ν and consider the non-dimensional quantity

$$s = -(x_d/u_\tau)\, du_\tau/dx_d. \tag{33}$$

Using

$$x = x_d u_\tau/\nu, \quad dx_d/dx = \nu/u_\tau(1-s), \tag{34}$$

(33) becomes

$$-s = (x/u_\tau)\,(du_\tau/dx)\,(1-s). \tag{35}$$

Let us assume tentatively that $s \to \infty$ as $x_d \to \infty$. Then

$$\frac{x}{u_\tau}\frac{du_\tau}{dx} \to 1, \quad u_\tau \to x \quad \text{or} \quad u_\tau \to \frac{x_d u_\tau}{\nu}, \tag{36}$$

which is impossible. On the other hand suppose $s \to 0$ as $x_d \to \infty$. Then

$$\frac{dx}{dx_d} \to \frac{u_\tau}{\nu}, \quad \frac{x_d}{x}\frac{dx}{dx_d} \to 1, \quad x \to \text{const.}\, x_d. \tag{37}$$

The constant in (37) must be a function of U_d and ν, so $u_\tau \to A_1 U_d$, where A_1 is a universal constant. But then the drag is independent of viscosity and this may be rejected on physical grounds. We conclude that $s \to s_0 = \text{const.}$ as $u_\tau \to u_{\tau 0}$. Integration of (33) then yields

$$u_{\tau 0} = A_d x_d^{-s}, \quad A_d = A U_d^{1-s} \nu^s, \tag{38}$$

where A is a universal constant, and we drop the subscript of s_0. Thus

$$U_0 = U_d/u_{\tau 0} = A_0 x^{s/(1-s)}, \tag{39}$$

where x and other mean quantities are scaled on $u_{\tau 0}$ and ν and A_0 is a universal constant.

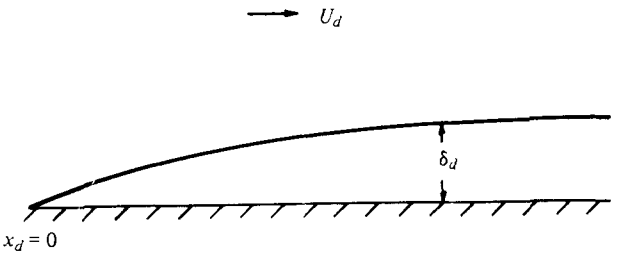

FIGURE 18. Flow over a flat plate at zero incidence.

Variation of boundary-layer thickness with distance along the plate

If an infinite plate moves with a suddenly imposed uniform stress, ρu_τ^2, the motion will cause the appearance and growth of a turbulent boundary layer over the plate whose thickness increases at an 'entrainment velocity' proportional, to first order, to the eddy velocity in the main portion of the layer which, from Reynolds number similarity, we assume to be proportional to u_τ. If we move with the mean position of the front we see an inflow of upper irrotational fluid into the turbulent region at a mean velocity equal to the entrainment velocity. In the present problem, the mean front is stationary at an angle θ to the horizontal and we conclude that there must be an inflow of irrotational fluid into the boundary layer with inflow velocity proportional to the local friction velocity. If we scale on U_d and ν, the boundary condition becomes†

$$-\frac{\partial\phi}{\partial n} = -\frac{\partial\phi}{\partial\xi}\sin\theta + \frac{\partial\phi}{\partial\eta}\cos\theta = K_0 U^{-1} \quad \text{at} \quad \eta = f(\xi), \quad U = U_d/u_\tau, \tag{40}$$

where $\mathbf{n}$ is the inward normal at the mean position of the interface $\eta = f(\xi)$, and ξ, η are the new co-ordinates, $\xi = x_d U_d/\nu$, $\eta = z_d U_d/\nu$. The velocity potential is ϕ and K_0 is a universal constant. One possibility is that $\phi = -\xi$ so that the boundary layer has no 'blocking' effect on the outside flow and the inward velocity is $U_d \sin\theta$. We should not assume this, however, and, in fact, it may be shown that the vertical velocity in the vicinity of the interface is not zero. In any case we are safe to use Reynolds number similarity to assume that, if it is not zero, it is of order u_τ, or, to first order, $u_{\tau 0} \propto x_d^{-s}$. If we take for ϕ,

$$\phi = \mathrm{Re}\,\alpha(\xi + i\eta)^a - \xi, \tag{41}$$

we get

$$\phi = \alpha_r \xi^a - a\alpha_i \eta \xi^{a-1} - \xi, \tag{42}$$

where α_r and α_i are real. Also, to first order, $\sin\theta = f'$ and $\cos\theta = 1$, so that (40) becomes

$$f'(1 - \alpha_r a\xi^{a-1} + \ldots) - a\alpha_i \xi^{a-1} \ldots \cong K_1 \xi^{-s},$$

where we have used (39). Thus $f' = K_2 \xi^{-s}$, $a = 1 - s$ and we verify that the vertical velocity is of order $u_{\tau 0}$ or less in the outer region of the boundary layer. It is also

† We neglect the weak mean vorticity above the front associated with the presence of fluid with vorticity (boundary-layer fluid above the mean position of the front) accompanying turbulent fluctuations. This region of vorticity is assumed to become negligibly thin compared with δ_d as $x_d \to \infty$, $\delta_d \to \infty$.

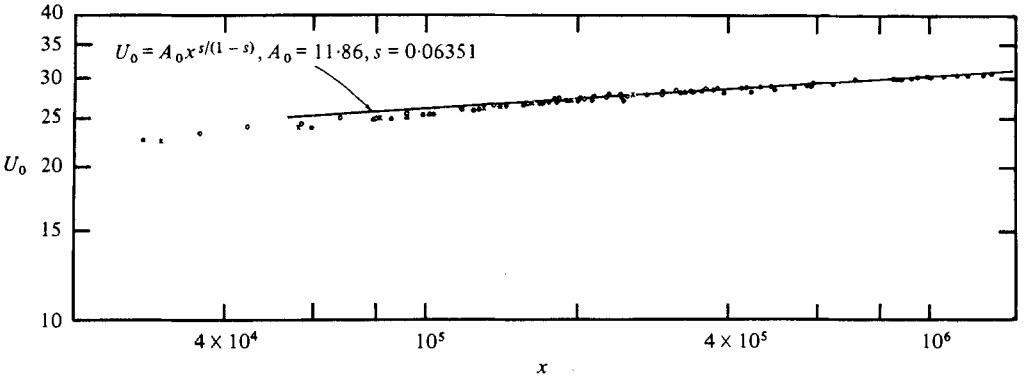

FIGURE 19. The drag law in a boundary layer. ●, Smith & Walker; ×, Schultz-Grunow; ○, Wieghardt.

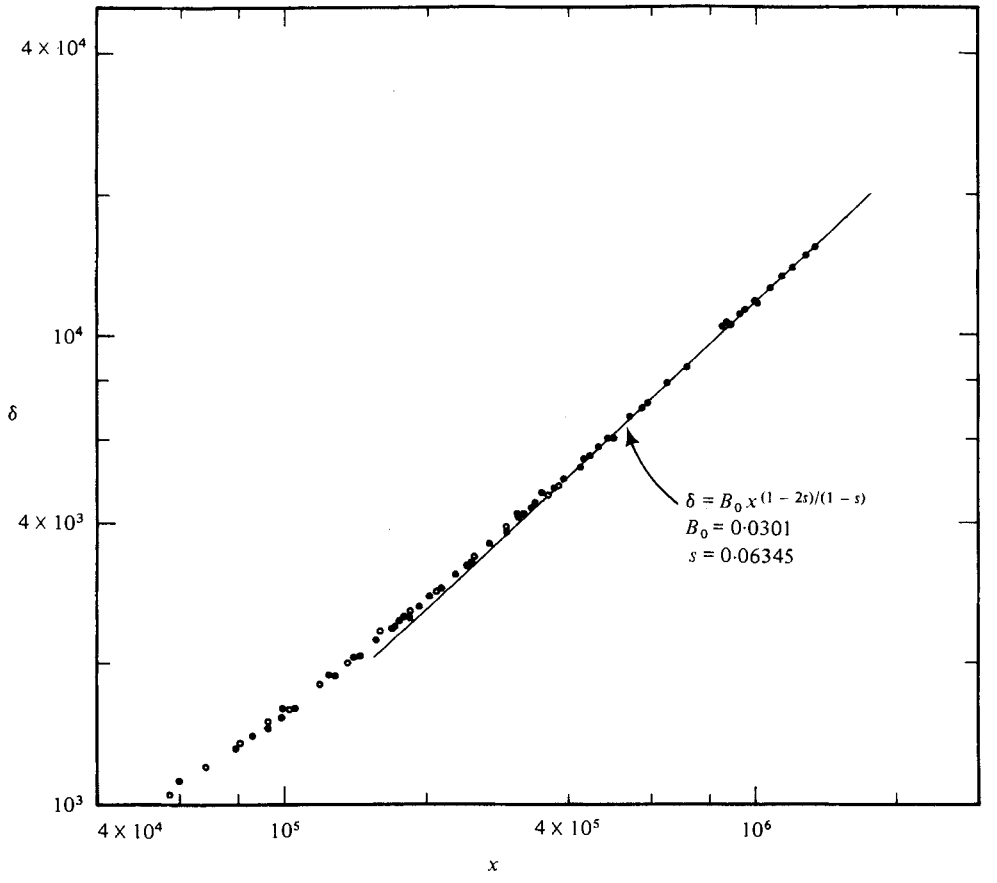

FIGURE 20. Boundary-layer thickness as a function of distance along the plate. ●, Smith & Walker; ○, Wieghardt.

independent of height in this region. We may go on to higher approximations, but this is sufficient for present purposes.

If we revert now to the scaling on $u_{\tau 0}$ and ν, $f' = K_2 \xi^{-s}$ has the integral

$$\delta_0 = B_0 x^{(1-2s)/(1-s)}, \quad \delta_0 = \delta_{d0} u_{\tau 0}/\nu, \quad x = x_d u_{\tau 0}/\nu, \tag{43}$$

where B_0 is a universal constant and δ_0 is the Reynolds number in a form analogous to that for a pipe. The predictions of (39) and (43) may be compared to figures 19 and 20. The empirical constant s was evaluated separately for the two sets of data and the agreement that $s \cong 0{\cdot}0635$ for both cases is reassuring.

Mean velocity distribution in the boundary layer

In a pipe the mean velocity profile is logarithmic in the region $1 \ll z \ll R^{\frac{1}{2}}$ and also in $R^{\frac{1}{2}} \ll z \ll R$ but the slopes of the curves in a plot of $\overline{u}$ *vs.* $\ln z$ are somewhat different and we have found that close inspection of the data revealed a transition region at $z \sim R^{\frac{1}{2}}$ and confirmed the existence of the mesolayer. In a turbulent boundary layer the theory is quite different, as we might expect from the new drag law in (39) which does not have the logarithmic behaviour of classical theory.

The distribution of $\overline{u}$ in the boundary layer is obtained to first order by matching. The inner form is

$$\overline{u} = u_+(z) + h_0(\delta_0)\, u_*(\hat{z}). \tag{44}$$

In (44), we scale on $u_{\tau 0}$ and ν and $\hat{z} = z/m(\delta_0)$, where we suspect, but do not require, that $m = \delta_0^{\frac{1}{2}}$. The outer form, assuming Reynolds-number similarity, is

$$U_0 - \overline{u} = u_0(\zeta), \quad \zeta = z/\delta_0. \tag{45}$$

Matching and using (39) and (43), we get

$$K_{00}\delta_0^{\alpha} - u_+(z) - h_0 u_*(\hat{z}) = u_0(\zeta), \tag{46}$$

where K_{00} is a universal constant and $\alpha = s/(1-2s)$. We find $h_0 = \delta_0^{\alpha}$ and that u_+ and $h_0 u_*$ are both of order δ_0^{α} in the mesolayer. The mean equations of motion then yield $m = \delta_0^{\frac{1}{2}}$ by equating the viscous term of order δ_0^{α}/m^2 to the inertia term of order $\delta_0^{2\alpha}/x$ in the mesolayer. The results of matching

$$U_0 - u_+(z) - \delta_0^{\alpha} u_*(\hat{z}) = u_0(\zeta), \quad \hat{z} = z/\delta_0^{\frac{1}{2}}, \tag{47}$$

are

$$u_+ = A_{00}^+ z^{2\alpha} + A_{01}^+ \quad (z \gg 1), \tag{48}$$

$$u_* = -A_{00}^+ \hat{z}^{2\alpha} + K_{00} - A_{10}\hat{z}^{-2\alpha} \quad (\hat{z} \gg 1), \tag{49}$$

$$u_0 = A_{10}\zeta^{-2\alpha} + A_{11} \quad (\delta_0^{-\frac{1}{2}} \ll \zeta \ll 1), \tag{50}$$

$$U_0 = K_{00}\delta_0^{\alpha} + A_{11} + A_{01}^+ \quad (\delta_0 \gg 1). \tag{51}$$

In contrast to classical results (Monin & Yaglom 1971, p. 314) we see that logarithmic behaviour is entirely absent in the mesolayer theory of the boundary layer. The mean velocity in (48) is appropriate to the region $1 \ll z \ll \delta_0^{\frac{1}{2}}$ below the mesolayer, and the velocity defect in (50) to the region $\delta_0^{\frac{1}{2}} \ll z \ll \delta_0$ above the mesolayer. We have seen that $s \cong \frac{1}{16}$, $\alpha \cong \frac{1}{14}$ so that the behaviour is close to logarithmic, but we should nevertheless explain why the classical argument is faulty. In classical theory one assumes that the velocity defect is independent of Reynolds number δ_0 in the

outer region and that it obeys the law of the wall in the inner region. The matching then yields logarithmic behaviour for U_0 and $\bar{u}$ in the matched region. In mesolayer theory, the matching is different, but even so in a pipe, for example, we have seen that logarithmic behaviour is found for U_0 and for $\bar{u}$ above and below the mesolayer. In the latter region of the pipe one may also argue that $\bar{u}_+$ is the mean velocity above the sublayer for flow in infinite half-space at the given friction velocity and therefore, from dimensional analysis, $d\bar{u}_+/dz \sim z^{-1}$. Integration yields $\bar{u}_+ \sim \ln z$. Let us show that the dimensional argument cannot be used successfully for the boundary layer. Looked at more carefully, the argument for the pipe is (1) that there is a region near the wall ($0 \leqslant z_d \ll a$ in classical theory, $0 \leqslant z_d \ll aR^{\frac{1}{2}}$ in mesolayer theory) in which there is a relation

$$f(d\bar{u}_d/dz_d, u_\tau, z_d, \nu) = 0 \tag{52}$$

and (2) that at larger z_d in this region ($\nu/u_\tau \ll z_d \ll a$ in classical theory,

$$\nu/u_\tau \ll z_d \ll R^{\frac{1}{2}}\nu/u_\tau$$

in mesolayer theory), viscosity may be neglected and therefore that

$$f_1(d\bar{u}_d/dz_d, u_\tau, z_d) = 0 \tag{53}$$

to first order, i.e.

$$d\bar{u}_d/dz_d \sim u_\tau z_d^{-1} \tag{54}$$

in this region. But notice that a dimensional argument that $f_1(Q_1, Q_2, \ldots, Q_n) = 0$ reduces to $f_2(Q_1, Q_2, \ldots, Q_{n-1}) = 0$ as $Q_n \to 0$ can only be justified if, in the limiting process involved in $Q_n \to 0$, no other Q_i tends to zero or infinity. In the boundary layer, however, we cannot keep the other quantities in (52) finite as $\nu \to 0$. We may show this as follows: If we choose a fixed δ_d and a fixed $z_d \ll \delta_d$, we may so vary U_d (or keep it fixed) as to satisfy the requirement $z_d/(\nu/u_\tau) \gg 1$ as $\nu \to 0$. but we must also require $z_d/(\nu/u_\tau)\,\delta^a \ll 1$ or $z_d/(\nu/u_\tau)^{1-a}\,\delta_d^a \ll 1$ as $\nu \to 0$, where $\delta = \delta_d u_\tau/\nu$, and where $(\nu/u_\tau)\,\delta^a$ is the mesolayer thickness ($a = 1$ in classical theory, $a = \frac{1}{2}$ in mesolayer theory). In classical theory, the two requirements are possible, but in mesolayer theory they are not and the argument leading to logarithmic behaviour fails.

It is not surprising in view of the form of the mean velocity in (48) and (50) that the mesolayer stands out more clearly in the boundary layer than in a pipe and this is so apparent, for example, in the plot of the boundary-layer data of Smith & Walker (1959) in the survey paper of Rotta (1962, see his figure 13.3) that it is astonishing that no mention is made of the damage that this does to the classical theory. The data we have now accumulated for the boundary layer includes some forty experiments† by Smith & Walker (1959), twenty experiments by Wieghardt (1969), one experiment by Klebanoff (1954) and one experiment by Ludwieg & Tillman (1950). We show a few of these in figures 21–27 and these and all other experiments reveal the same qualitative behaviour as in a pipe or in figure 11. Figures 21 and 22 show individual plots at very different Reynolds numbers. Both show the behaviour of figure 11 and a great difference of z for the two transition regions. Figures 23–25 show individual experiments over wide ranges of Reynolds number by Smith & Walker and Wieghardt and figure 26 shows that the deviation from logarithmic behaviour cannot be ascribed to experi-

† In the figures for the boundary layer we often use R instead of δ_0 for the non-dimensional boundary-layer thickness.

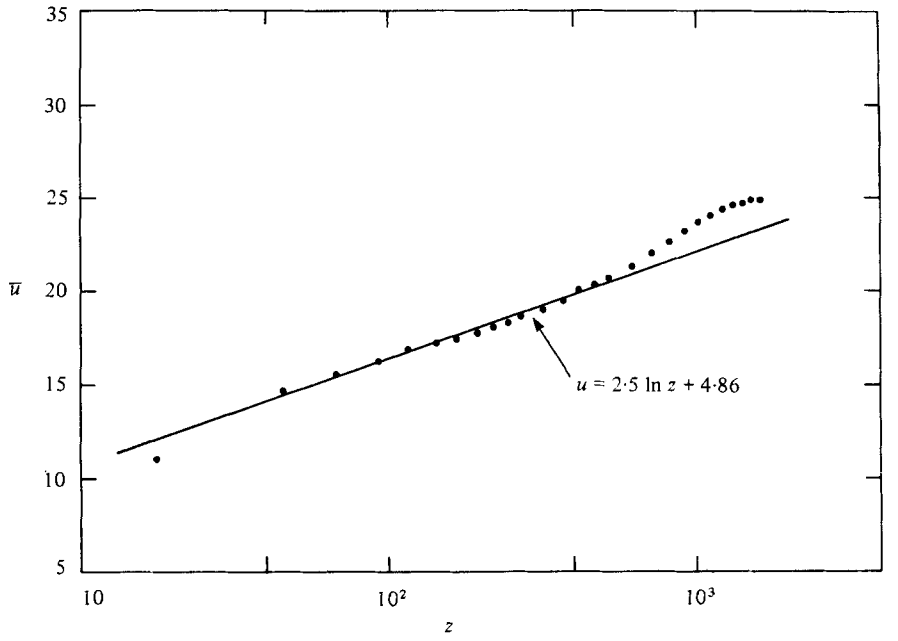

FIGURE 21. Mean velocity in a boundary layer at low Reynolds number (Smith & Walker 1959). $R = 1326$.

mental error. Figure 27 shows similar behaviour in the data of Ludwieg & Tillman. We evaluated the constants in the first two terms of the inner expansion $\bar{u}_+$ by assuming that this is a good expression for $\bar{u}$ in the region $15 < z < 0{\cdot}7R^{\frac{1}{2}}$. The results, using the data of Smith & Walker, are in figure 28. Certainly, the observed velocity shear is greater than $\partial\bar{u}_+/\partial z$ somewhere near the wall and smaller than $\partial\bar{u}_+/\partial z$ far away from the wall. The theory shows that $\partial\bar{u}/\partial z = \partial\bar{u}_+/\partial z$ at a point in the mesolayer, i.e. at a distance proportional to $\delta_0 = R^{\frac{1}{2}}$. It is rather difficult to locate this point in any given experiment but the estimates from all experiments are shown in figure 29 and it is altogether quite convincing that there is the predicted variation. Finally, using the expression for $\bar{u}_+$ and

$$\bar{u} = \bar{u}_+ + \delta_0^{\alpha} u_*(\hat{z}), \tag{55}$$

we could plot $(\bar{u} - \bar{u}_+)\,\delta_0^{-\alpha}$. We see in figure 30 that this quantity is, in fact, a function of $\hat{z}$ alone in accordance with theory.

7. The Ekman layer

The neutral planetary boundary layer, or Ekman layer, offers an interesting application of mesolayer theory. For present purposes, we idealize it as the flow of a liquid over a rotating smooth plate at $z = 0$. The velocity in the relative frame (u_g, v_g) at $z \to \infty$ is called the geostrophic velocity and is assumed constant. The mean equations, scaled on inner variables ν and u_τ, are (Plate 1971)

$$-R^{-1}(\bar{v} - v_g) = \bar{u}_{zz} + T_z, \tag{56}$$

$$R^{-1}(\bar{u} - u_g) = \bar{v}_{zz} + Q_z, \tag{57}$$

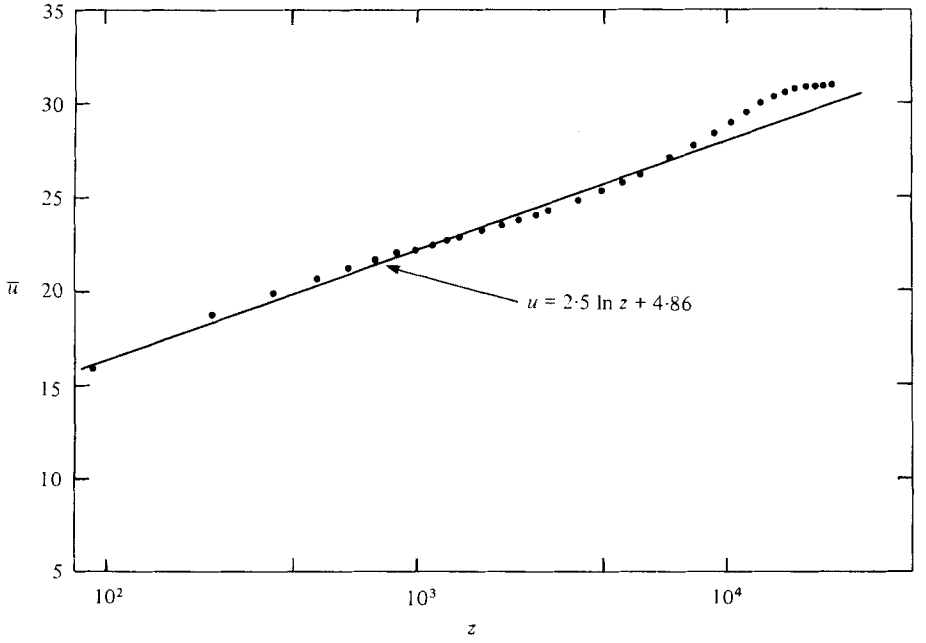

FIGURE 22. Mean velocity in a boundary layer at high Reynolds number (Smith & Walker 1959). $R = 15466$.

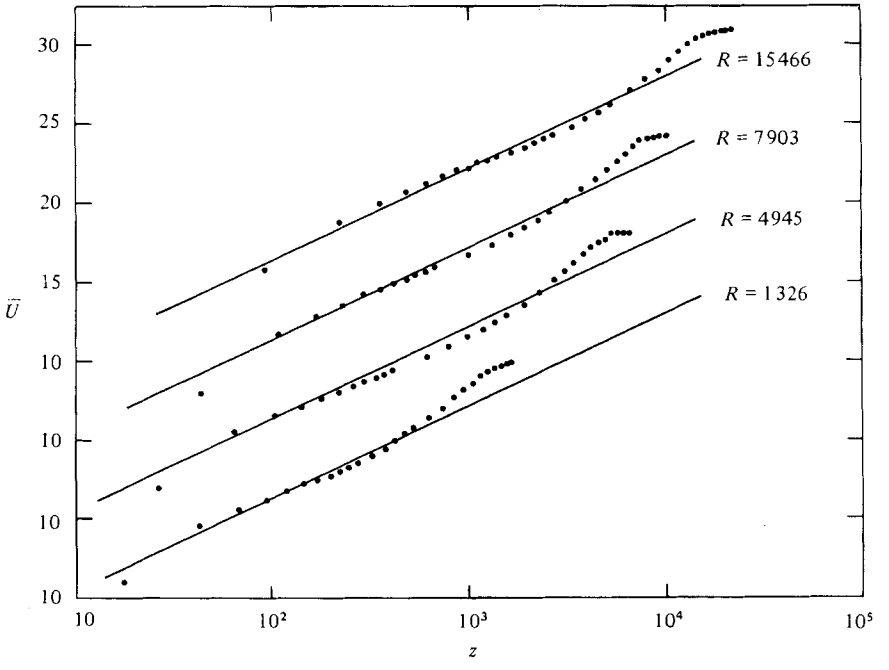

FIGURE 23. Mean velocity in a boundary layer over a range of Reynolds numbers (Smith & Walker 1959).

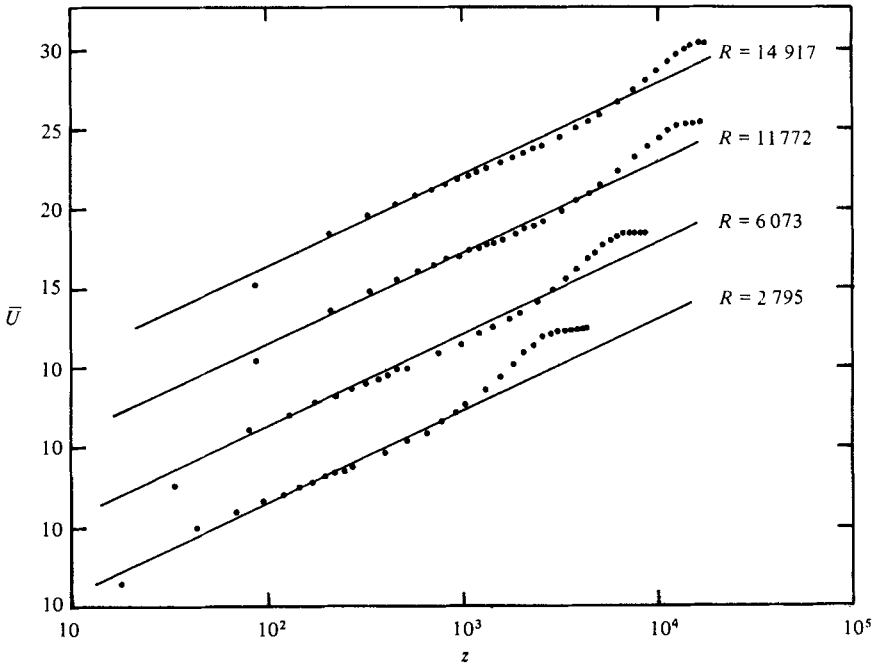

FIGURE 24. Mean velocity in a boundary layer over a range of Reynolds numbers (Smith & Walker 1959).

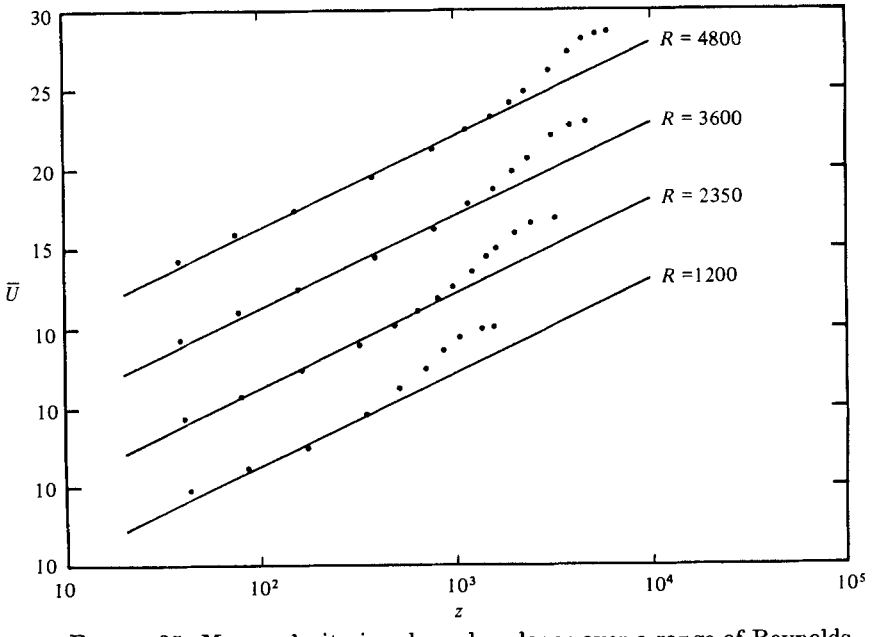

FIGURE 25. Mean velocity in a boundary layer over a range of Reynolds numbers (Wieghardt 1969).

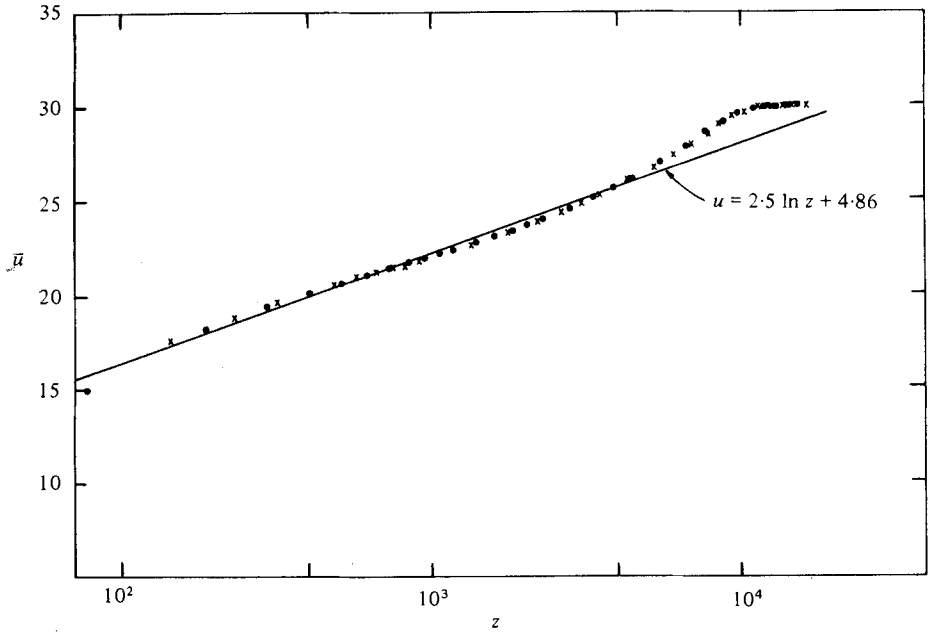

FIGURE 26. Mean velocity in a boundary layer at two similar Reynolds numbers (Smith & Walker 1959). ●, R ($= u_\tau \delta_d/\nu$) = 10587; ×, R = 10522.

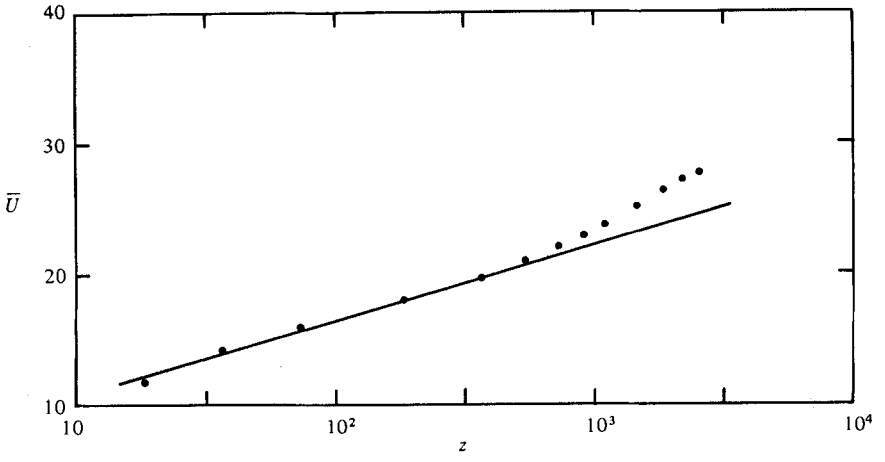

FIGURE 27. Mean velocity in a boundary layer (Ludwieg & Tillmann 1950). R = 2600.

where we adopt, initially, a co-ordinate system with axes of arbitrary orientation in the x,y plane. The Reynolds number is now $R = u_\tau^2/fv$, where f is the Coriolis parameter, or twice the angular speed of the rotating system. The two Reynolds stresses are $T = -\overline{u'w'}$ and $Q = -\overline{v'w'}$.

The problem was approached from the viewpoint of classical theory independently by Gill (1967) and Csanady (1967). They assumed a co-ordinate system with x axis in

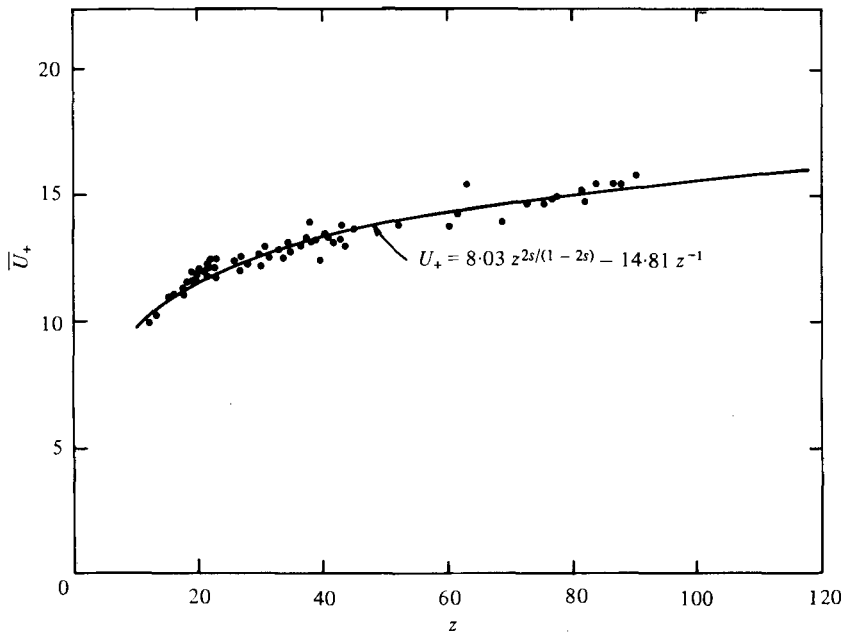

FIGURE 28. Calculation of the coefficients in the expression for $\bar{u}_+$.

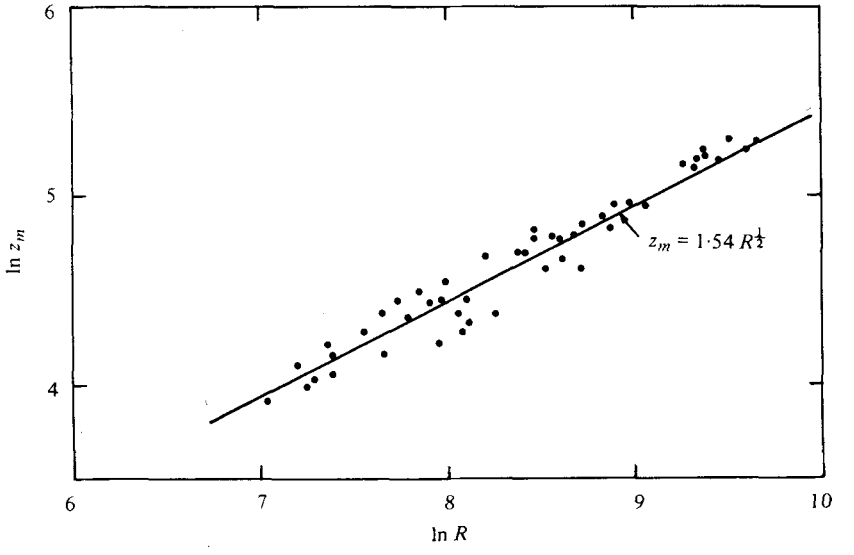

FIGURE 29. Distance of transition region from the wall in boundary-layer experiments.

the direction of the surface stress of magnitude ρu_τ^2 and argued that there should be a region near the wall where

$$\overline{u} = \overline{u}_+(z), \quad \overline{v} = 0. \tag{58}$$

They further argued that velocity defects $\overline{u} - u_g$ and $\overline{v} - v_g$ should obey Reynolds-number similarity in the outer region. If the planetary boundary layer has a finite

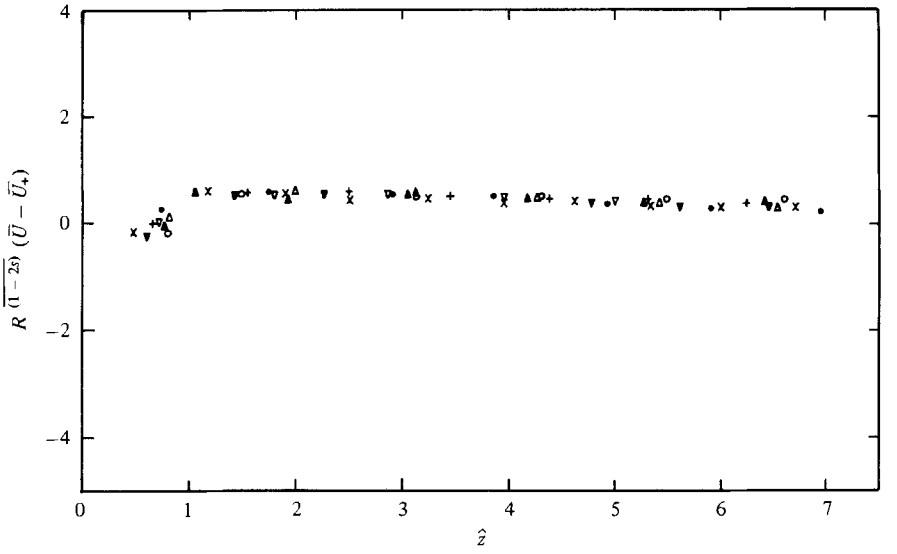

FIGURE 30. Plot of $(\bar{u}-\bar{u}_+)\,R^{-\alpha}$ in (51). ×, 1326; ○, 2659; +, 4687; ▲, 6069; ▼, 10522; ▽, 10587; △, 11772; ●, 15446.

depth H, it should be proportional to u_τ/f and this was used for the outer length.† The outer behaviour is then

$$\bar{u}-u_g = u_0(\zeta), \quad \bar{v}-v_g = v_0(\zeta), \quad \zeta = z/R. \tag{59}$$

A matching of (58) and (59) in the overlap region yields the classical results that the 'geostrophic' drag is logarithmic and that the mean velocity profile near the ground is logarithmic as in non-rotating shear flow in a pipe. Much effort has gone into an attempt to verify the geostrophic drag law because of its practical importance in numerical weather forecasting and atmospheric modelling.

If we now go over to mesolayer theory, then, as in pipe flow, we may now express quantities near the surface as follows:

$$\bar{u}_z = f_+(z)+h_1(R)f_*(\hat{z})+\ldots, \tag{60}$$

$$\bar{v}_z = g_+(z)+h_2(R)g_*(\hat{z})+\ldots, \tag{61}$$

$$T = T_+(z)+l_1(R)T_*(\hat{z})+\ldots, \tag{62}$$

$$Q = Q_+(z)+l_2(R)Q_*(\hat{z})+\ldots, \tag{63}$$

where the similarity variable $\hat{z} = z/m$ and where we suspect but do not require at this point that m is equal to $R^{\frac{1}{2}}$. Substitution into the derivatives of the equations of motion (56) and (57) then yields

$$-m^2R^{-1}(g_+ + h_2g_*) = l_1T_*'' + h_1f_*'', \quad T_+'' + f_+'' = 0, \tag{64}$$

$$m^2R^{-1}(f_+ + h_1f_*) = l_2Q_*'' + h_2g_*'', \quad Q_+'' + g_+'' = 0. \tag{65}$$

Since we have an arbitrary co-ordinate system, it is apparent from dimensional analysis that the inner mean velocity components are logarithmic so that f_+ and g_+ in

† Measurements (Plate 1971; Howroyd & Slawson 1975) give $H \cong 0{\cdot}4u_\tau/f$.

(60) and (61) are proportional to z^{-1} or $\hat{z}^{-1}m^{-1}$ in the mesolayer. Furthermore (64) and (65) evaluated at the plate lead to $h_1 = h_2 = m^2R^{-1}$. Then in (64) and (65) the g_+ and f_+ terms are small in the mesolayer and therefore we find that

$$h_1 = h_2 = l_1 = l_2 = 1, \tag{66}$$

and that $m = R^{\frac{1}{2}}$, as we anticipated. Finally the existence of the small terms, of relative order $R^{-\frac{1}{2}}$, represented by g_+ and f_+ in (64) and (65) suggest that in higher approximations for the mean quantities the functions of R decrease in increments of $R^{-\frac{1}{2}}$.

We may now write down the first three terms for the mean quantities in (60)–(63). They are

$$\bar{u}_z = f_+(z) + f_{*0}(\hat{z}) + R^{-\frac{1}{2}}f_{*1}(\hat{z}), \tag{67}$$

$$\bar{v}_z = g_+(z) + g_{*0}(\hat{z}) + R^{-\frac{1}{2}}g_{*1}(\hat{z}), \tag{68}$$

$$T = T_+(z) + T_{*0}(\hat{z}) + R^{-\frac{1}{2}}T_{*1}(\hat{z}), \tag{69}$$

$$Q = Q_+(z) + Q_{*0}(\hat{z}) + R^{-\frac{1}{2}}Q_{*1}(\hat{z}). \tag{70}$$

We assume Reynolds-number similarity for the outer forms to first approximation, for example $T \sim T_0(\zeta)$, and then the equations of motion suggest the higher approximations, e.g. $T = T_0(\zeta) + R^{-1}T_1(\zeta) + \ldots$. We now match and, using (64) and (65), obtain

$$f_+ = K_1z^{-1} + \alpha_1z^{-2}, \quad g_+ = K_2z^{-1} + \beta_2z^{-2}, \quad T_+ = a_1 - K_1z^{-1}, \quad Q_+ = a_2 - K_2z^{-1}, \tag{71}$$

$$f_{*0} = A_{02}\hat{z}^{-4} + A_{03}\hat{z}^{-6}, \quad f_{*1} = -K_1\hat{z}^{-1} + A_{12}\hat{z}^{-3}, \quad g_{*0} = B_{02}\hat{z}^{-4} + B_{03}\hat{z}^{-6},$$

$$g_{*1} = -K_2\hat{z}^{-1} + B_{12}\hat{z}^{-3}. \tag{72}$$

The outer forms are

$$\bar{u}_\zeta = 2E_{21} + 6E_{31}\zeta, \quad \bar{v}_\zeta = -2D_{21} - 6D_{31}\zeta, \quad T = a_1 + E_{01} + E_{11}\zeta, \quad Q = a_2 + D_{01} + D_{11}\zeta. \tag{73}$$

A remarkable feature of these solutions is the cancelling of the z^{-1} term in the first component of the mean velocity gradient by the mesolayer contribution. This means that the *velocity profile is no longer logarithmic above the mesolayer as it is, for example, in pipe flow.* This behaviour is in agreement with the integrals of (67) and (68) which indicate that the mesolayer contribution to the mean velocity exceeds, in order of magnitude, the contribution of the first component. This differs from the situation in a pipe where the contributions are of the same order. This large velocity in the mesolayer directly causes the geostrophic velocities to be $u_g \sim R^{\frac{1}{2}}, v_g \sim R^{\frac{1}{2}}$ which differ greatly from the logarithmic behaviour of the classical results (Plate 1971). Experiments with rotating wind tunnels (Caldwell, Van Atta & Holland 1972; Kreider 1973; Howroyd & Slawson 1975) provide a number of measurements which are presented in figure 31. The scatter is so great that we do not regard the results as conclusive but, certainly, the predicted behaviour is possible.

We may obtain additional theoretical information from the integral of (57), where we now take a co-ordinate system with x axis along the surface stress. We get

$$\int_0^\infty (\bar{u} - u_g)\,dz = 0. \tag{74}$$

This shows that $\bar{u}$ must exceed u_g over a large region, obviously the outer part of the

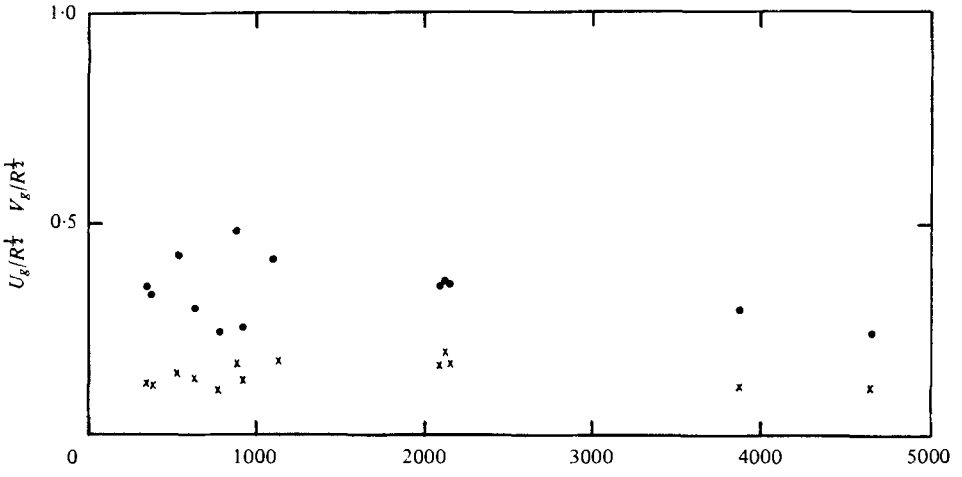

FIGURE 31. Experimental behaviour of geostrophic velocities as functions of R. ●, $U_g/R^{\frac{1}{2}}$; ×, $V_g/R^{\frac{1}{2}}$.

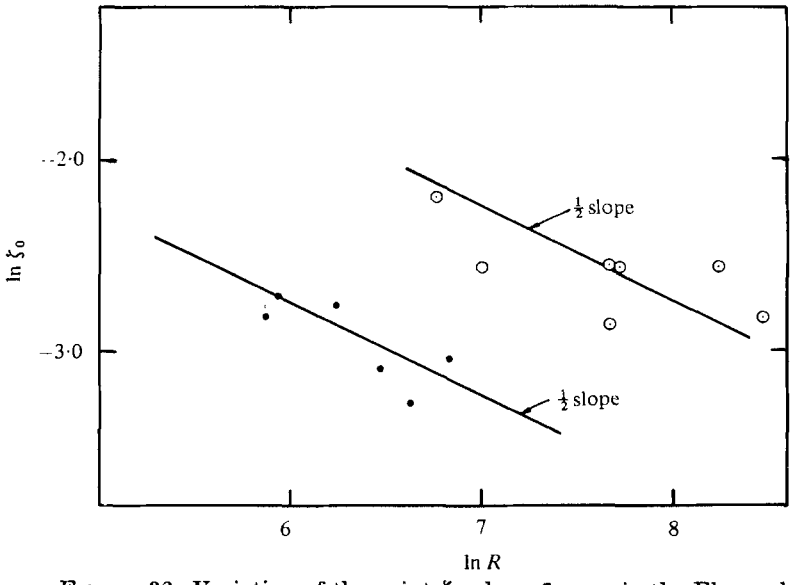

FIGURE 32. Variation of the point ζ_0 where $\bar{u} = u_g$ in the Ekman layer. ●, Kreider; ⊙, Caldwell *et al.*

layer because $\bar{u} < u_g$ in the lower portions. This prediction is confirmed by all experimental data. According to (57) when $\bar{u} - u_g = 0$, the Reynolds stress forces and viscous forces are equal and this is the fundamental property of the mesolayer. This predicts that $\bar{u} = u_g$ at a point $\zeta_0 \sim R^{-\frac{1}{2}}$ as indicated by the data in figure 32 although the scatter is great. Since $\bar{u} > u_g$ in the outer region where $\bar{u} - u_g$ is of order 1, and, since this region has a thickness of order R, the positive contribution to (74) is of order R. But then, because $\bar{u} < u_g$ in a small region of thickness of order $R^{\frac{1}{2}}$, we find that $\bar{u} - u_g$ is large of order $R^{\frac{1}{2}}$ in the mesolayer if we are to obtain an equal negative contribution to (74). This agrees with the above theory.

Physically, we anticipate that the mesolayer effect will be to increase the shear in

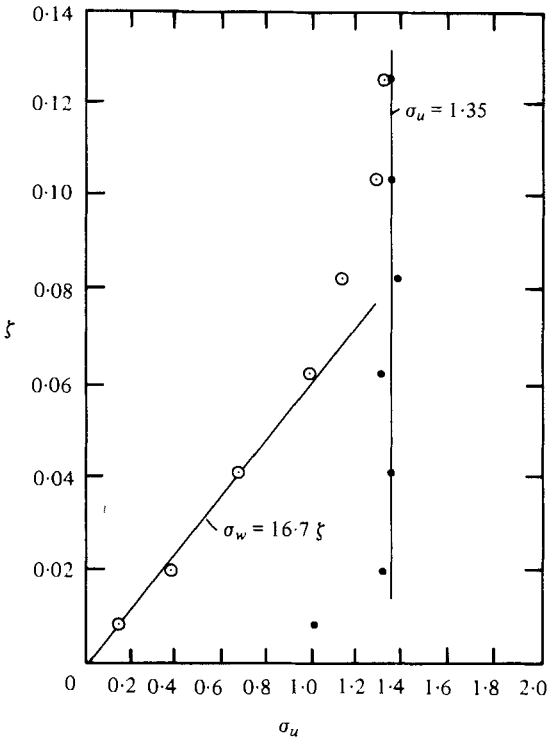

FIGURE 33. Plot of data of McDougall (1979) for r.m.s. horizontal and vertical velocities near a wall. We non-dimensionalize on 'action' K and total fluid depth H.

the lower portions of the mesolayer (to permit the $R^{\frac{1}{2}}$ velocities) and to decrease the shear in the upper portions of the mesolayer. We have already noted that the shear becomes zero as $\bar{u}$ reaches a maximum aloft and, in fact, the observations of Kreider (1973) indicate a layer of increased shear above a point fixed with respect to the sublayer at, perhaps, $z \sim 15$.

8. Grid turbulence near a wall

A recent paper by McDougall (1979) reported r.m.s. velocities near a wall in turbulence generated by an oscillating grid at some distance. This is a form of shear-free turbulence similar to that of Uzkan & Reynolds except that the r.m.s. velocities increase and length scales decrease with distance from the wall. As mentioned earlier, a theoretical model of grid turbulence (Long 1978*b*) predicts, for an infinite fluid,

$$\sigma_{du} = K/\xi_d, \quad l \sim \xi_d, \tag{75}$$

with distance ξ_d from the grid, where l is the integral scale and K is a constant called the 'action' of the grid. σ_{du} is an r.m.s. velocity, say the component parallel to the plane of the grid. In McDougall's experiment, $\sigma_{du} \cong 0{\cdot}34$ cm sec^{-1} at a distance of 10·0 cm from the grid so that $K = 3{\cdot}4$ cm^2 s^{-1}. The wall is located at $H = 12{\cdot}25$ cm from the grid and we compute $\sigma_{du} = 0{\cdot}28$ cm s^{-1} at this distance for the infinite fluid.

This is considerably less than 0·38 cm s^{-1} for the measured values near the wall so that the wall increases the r.m.s. horizontal velocities as it does in the wind-tunnel experiments. Application of mesolayer theory is simple in this problem. If we non-dimensionalize with K and H and take z_d as distance from the wall, we have

$$\sigma_u = \sigma_{u*}(\hat{z}), \quad \hat{z} = z/R^{\frac{1}{2}}, \quad z = z_d K/\nu H \quad (\hat{z} \sim 1), \tag{76}$$

$$\sigma_w = R^{-\frac{1}{2}}\sigma_{w*}(\hat{z}), \quad R = K/\nu \quad (\hat{z} \sim 1) \tag{77}$$

to first order, in the region near the wall, and

$$\sigma_u = u_0(\zeta), \quad \sigma_w = w_0(\zeta), \quad \zeta = z_d/H \quad (\zeta \sim 1) \tag{78}$$

far from the wall. Solutions for the matched region are

$$\sigma_u = A, \quad \sigma_w = B\zeta \quad (R^{-\frac{1}{2}} \ll \zeta \ll 1), \tag{79}$$

where A and B are universal constants. The predicted behaviour is seen in the data of figure 33, where $A \cong 1{\cdot}35$, $B \cong 16{\cdot}7$. We estimate the mesolayer to be of thickness

$$\delta_{dm} \cong 1{\cdot}5(\nu l/\sigma)^{\frac{1}{2}},$$

where σ and l are the velocity and horizontal length scales near the wall. The data give $\nu \cong 0{\cdot}01$, $l \cong 1{\cdot}0$, $\sigma \cong 0{\cdot}34$ so that $\delta_{dm} \cong 0{\cdot}26$ cm or $\zeta_m \cong 0{\cdot}02$. It is just here that the predicted constancy of σ_u begins as we see in figure 33.

This research was supported by the Office of Naval Research, Fluid Dynamics Division, under Contract N00014-76-C-0184 and by the National Science Foundation Grant Nos. ATM-7907026 and OCE 76-18887. We wish also to thank Dr C. S. Chern who compiled the data of figures 7 and 8 and who contributed to many of the ideas in the paper.

REFERENCES

ADRIAN, R. J. & FERREIRA, R. T. S. 1979 Higher order moments in turbulent thermal convection. *2nd Symp., Turbulent Shear Flows, Imperial College*. 12·1–12·6.

AFZAL, N. 1976 Millikan's argument at moderately large Reynolds number. *Phys. Fluids* **19**, 600–602.

AFZAL, N. & YAJNIK, K. 1973 Analysis of turbulent pipe and channel flows at moderately large Reynolds numbers. *J. Fluid Mech.* **61**, 23–31.

BATCHELOR, G. K. 1967 *An Introduction to Fluid Mechanics*. Cambridge University Press.

BULLOCK, K. J., COOPER, R. E. & ABERNATHY, F. H. 1978 Structural similarity in radial correlations and spectra of longitudinal velocity fluctuations in pipe flow. *J. Fluid Mech.* **88**, 585–608.

BUSH, W. B. & FENDELL, F. E. 1972 Asymptotic analysis of turbulent channel and boundary-layer flow. *J. Fluid Mech.* **56**, 657–681.

BUSH, W. B. & FENDELL, F. E. 1973 Asymptotic analysis of turbulent channel flow for mean turbulent energy closures. *Phys. Fluids* **16**, 1189–1197.

BUSH, W. B. & FENDELL, F. E. 1974 Asymptotic analysis of turbulent channel flow for mixing length theory. *SIAM, J. Appl. Math.* **26**, 314–427.

BUSINGER, J. A., WYNGAARD, J. C., ISUMI, Y. & BRADLEY, E. F. 1971 Flux profile relationships in the atmospheric surface layer. *J. Atmos. Sci.* **28**, 181–189.

CALDWELL, D. R., VAN ATTA, C. W. & HOLLAND, K. N. 1972 A laboratory study of the turbulent Ekman layer. *Geophys. Fluid Dynamics* **3**, 125–160.

CHEN, C. H. & BLACKWELDER, R. F. 1978 Large-scale motion in a turbulent boundary layer: A study using temperature contamination. *J. Fluid Mech.* **89**, 1–31.

CHERN, C. S. & LONG, R. R. 1980 A new theory of turbulent thermal convection over heated surfaces. (Unpublished manuscript.)

CSANADY, G. T. 1967 On the resistance law of a turbulent Ekman layer. *J. Atmos. Sci.* **24**, 467–471.

DEARDORFF, J. W. & WILLIS, G. F. 1967 Investigation of turbulent thermal convection between horizontal plates. *J. Fluid Mech.* **28**, 675–704.

FALCO, R. E. 1974 Some comments on turbulent boundary layer structure inferred from the movements of a passive contaminant. *A.I.A.A. Paper* no. 74–99.

FALCO, R. E. 1977 Coherent motions in the outer region of turbulent boundary layers. *Phys. Fluids* **20**, S124–132.

FALCO, R. E. 1978 An experimental study of Reynolds stress producing motions in the outer part of turbulent boundary layers, Part I. The shape, scale, evolution and Reynolds number dependence. (Unpublished manuscript.)

FENDELL, F. E. 1972 Singular perturbation and turbulent shear layers near walls. *J. Astro. Sci.* **20**, 129–165.

FERREIRA, R. T. D. 1978 Unsteady turbulent thermal convection. Ph.D. thesis, Dept. Mech. Engng., University of Illinois.

FRITSCH, W. 1928 Einfluss der Wandrauhigkeit auf die turbulente Geschwindigkeit-Verteilung in Rinnen. *Z. angew. Math. Mech.* **8**, 199–216.

GILL, A. E. 1967 The turbulent Ekman layer. (Unpublished manuscript.)

GLOBE, S. & DROPKIN, D. 1959 Natural convection heat transfers in liquids confined by two horizontal plates and heated from below. *J. Heat Transfer* **81**, 24–28.

GUPTA, A. K. & KAPLAN, R. E. 1972 Statistical characteristics of Reynolds stress in a turbulent boundary layer. *Phys. Fluids* **15**, 981–895.

GUPTA, A. K., LAUFER, J. & KAPLAN, R. E. 1971 Spatial structure in the viscous sublayer. *J. Fluid Mech.* **50**, 493–512.

HINZE, J. O. 1975 *Turbulence.* McGraw-Hill.

HISHIDA, M. & NAGONO, Y. 1979 Structure of turbulent velocity and temperature fluctuation in fully developed pipe flow. *J. Heat Transfer* **101**, 15–22.

HOPFINGER, E. J. & TOLY, J.-A. 1976 Spatially decaying turbulence and its relation to mixing across density interfaces. *J. Fluid Mech.* **78**, 155–175.

HOWROYD, G. C. & SLAWSON, P. R. 1975 The characteristics of a laboratory produced turbulent Ekman layer. *Boundary Layer Met.* **8**, 201–219.

HUNT, J. C. R. & GRAHAM, J. M. R. 1978 Free-stream turbulence near plane boundaries. *J. Fluid Mech.* **84**, 209–235.

IZAKSON, A. 1937 Formula for the velocity distribution near a wall. *Zh. Eksper. Teor. Fiz.* **7**, 919–924.

KÁRMÁN, T. VON 1930 Mechanische Ähnlichkeit und Turbulenz. *Nachr. Ges. Wiss. Göttingen, Math.-Phys. Kl.*, 58–76.

KLEBANOFF, R. S. 1954 Characteristics of turbulence in a boundary layer with zero pressure gradient. *N.A.C.A. TN* 3178.

KLINE, S. J., REYNOLDS, W. C., SCHRAUB, F. A. & RUNSTADLER, P. W. 1967 The structure of turbulent boundary layer. *J. Fluid Mech.* **30**, 741–772.

KORNEYEV, A. L. & SEDOV, L. I. 1976 Theory of isotropic turbulence and its comparison with experimental data. *Fluid Mechanics, Soviet Research* 5, No. 5, 37–48.

KREIDER, J. F. 1973 *A Laboratory Study of the Turbulent Ekman Layer.* Ph.D. Thesis, College of Engineering, University of Colorado, Boulder.

LAUFER, J. 1954 The structure of turbulence in fully developed pipe flow. *Nat. Advis. Comm. Aeronautics*, Rep. No. 1174.

LAUFER, J. 1975 New trends in experimental turbulence research. *Ann. Rev. Fluid Mech.* **7**, 307–326.

LAWN, C. J. 1971 The determination of the rate of dissipation in turbulent pipe flow. *J. Fluid Mech.* **48**, 477–505.

LONG, R. R. 1976 Relation between Nusselt number and Rayleigh number in turbulent thermal convection. *J. Fluid Mech.* **73**, 445–451.

LONG, R. R. 1978*a* The decay of turbulence. Tech. Rep. No. 13 (Series C). The Johns Hopkins University.

LONG, R. R. 1978*b* Theory of turbulence in a homogeneous fluid induced by an oscillating grid. *Phys. Fluids* **21**, 1887–1888.

LONG, R. R. 1980*a* A new theory of turbulent flow in a pipe. (Unpublished manuscript.)

LONG, R. R. 1980*b* A new theory of the turbulent boundary layer in zero pressure gradient. (Unpublished manuscript.)

LONG, R. R. 1980*c* A new theory of the neutral planetary boundary layer. (Unpublished manuscript.)

LONG, R. R. 1980*d* On the energy spectrum at higher wave numbers. (Unpublished manuscript.)

LUDWIEG, H. & TILLMANN, W. 1950 Investigations of the wall shearing stress in turbulent boundary layers. *N.A.C.A.* TM 1285.

LUND, K. O. & BUSH, W. B. 1980 Asymptotic analysis of plane turbulent Couette–Poiseuille flows. *J. Fluid Mech.* **96**, 81–104.

MALKUS, W. V. R. 1979 Turbulent velocity profiles from stability criteria. *J. Fluid Mech.* **90**, 401–414.

MCDOUGALL, T. J. 1979 Measurements of turbulence in a zero-mean shear mixed layer. *J. Fluid Mech.* **94**, 409–431.

MILLIKAN, C. B. 1938 A critical discussion of turbulent flows in channels and circular tubes. *Proc. 5th Int. Cong. Appl. Mech., Cambridge (USA).*

MITCHELL, J. E. & HANRATTY, T. J. 1966 A study of turbulence at a wall using an electrochemical wall shear-stress meter. *J. Fluid Mech.* **26**, 199–221.

MONIN, A. S. & YAGLOM, A. M. 1971 *Statistical Fluid Mechanics. I. Mechanics of Turbulence.* Massachusetts Institute of Technology Press.

NYCHAS, S. G., HERSHEY, H. S. & BRODKEY, M. P. 1973 A visual study of turbulent shear flow. *J. Fluid Mech.* **61**, 513–540.

NIKURADSE, J. 1932 Gesetzmässigkeiten der turbulenten Strömung in glatten Rohren. *Forsch. Arbeiten Ing.-Wesen*, No. 356.

PERRY, A. E. & ABELL, C. J. 1975 Scaling laws for pipe flow turbulence. *J. Fluid Mech.* **67**, 257–271.

PERRY, A. E. & ABELL, C. J. 1977 Asymptotic similarity of turbulence structure in smooth-and-rough-walled pipes. *J. Fluid Mech.* **79**, 785–791.

PLATE, E. J. 1971 *Aerodynamic Characteristics of the Atmospheric Boundary Layers.* U.S. Atomic Engng Comm.

PRANDTL, L. 1925 Bericht über Untersuchungen zur ausgebildeten Turbulenz. *Z. angew. Math. Mech.* **5**, No. 2, 136–139.

PRANDTL, L. 1932 Zur turbulenten Strömung in Röhren und läns Platten. *Ergebn. Aerodyn. Versuchsanst., Göttingen* **4**, 18–29.

RAO, K., NARAHARI, NARASIMHA, R. & NARAYANAN, M. A. B. 1971 The 'bursting' phenomenon in a turbulent boundary layer. *J. Fluid Mech.* **48**, 339–352.

ROTTA, J. C. 1962 Turbulent boundary layers in incompressible flow. *Progress in Aeronautical Sciences* **2**, 1–220.

SCHILDKNECHT, M., MILLER, J. A. & MEIR, G. E. A. 1979 The influence of suction on the structure of turbulence in fully developed pipe flow. *J. Fluid Mech.* **90**, 67–107.

SMITH, D. W. & WALKER, J. H. 1959 *Skin-friction measurements in incompressible flow.* NASA Rep. R-26.

SOMERSCALES, E. F. C. & GAZDA, I. W. 1969 Thermal convection in high Prandtl number liquids at high Rayleigh numbers. *Int. Heat and Mass Transfer* **12**, 1491–1511.

TENNEKES, H. 1968 Outline of a second-order theory of turbulent pipe flow. *A.I.A.A. J.* **6**, 1735–1740.

TENNEKES, H. & LUMLEY, J. L. 1972 *A First Course in Turbulence.* Massachusetts Institute of Technology Press.

THEODORSEN, T. 1955 The structure of turbulence. 50 *Jahre Grenzschichtforschung* (ed. H. Görtler & W. Tollmien). Braunschweig: Vieweg und Sohn.

THEODORSEN, T. 1962 The structure of turbulence. In *Fluid Dynamics and Applied Mathematics* (ed. J. B. Diaz & S. I. Pai). Gordon and Breach.

THOMAS, N. H. & HANCOCK, D. E. 1977 Grid turbulence near a moving wall. *J. Fluid Mech.* **82**, 481–496.

THOMAS, D. B. & TOWNSEND, A. A. 1957 Turbulent convection over a heated horizontal surface. *J. Fluid Mech.* **2**, 473–492.

THOMPSON, S. M. & TURNER, J. S. 1975 Mixing across an interface due to turbulence generated by an oscillating grid. *J. Fluid Mech.* **67**, 349–368.

TOWNSEND, A. A. 1976 *The Structure of Turbulent Shear Flow.* Cambridge University Press.

TRITTON, D. J. 1967 Some new correlation measurements in a turbulent boundary layer. *J. Fluid Mech.* **28**, 439–462.

UEDA, H. & MIZUSHINA, T. 1977 Turbulence structure in the inner part of the wall region in a fully developed turbulent tube flow. *Proc. 5th Biennial Symp. on Turb., Univ. Missouri, Rolla.*

UZKAN, T. & REYNOLDS, W. C. 1967 A shear-free turbulent boundary layer. *J. Fluid Mech.* **28**, 803–821.

WIEGHARDT, K. 1969 Computation of turbulent boundary layer. *Proc.* 1968 *AFOSR-IFP Stanford Conf.*, vol. 2 (ed. D. E. Coles & E. A. Hirst).

YAJNIK, K. S. 1970 Asymptotic theory of turbulent shear flows. *J. Fluid Mech.* **42**, 411–427